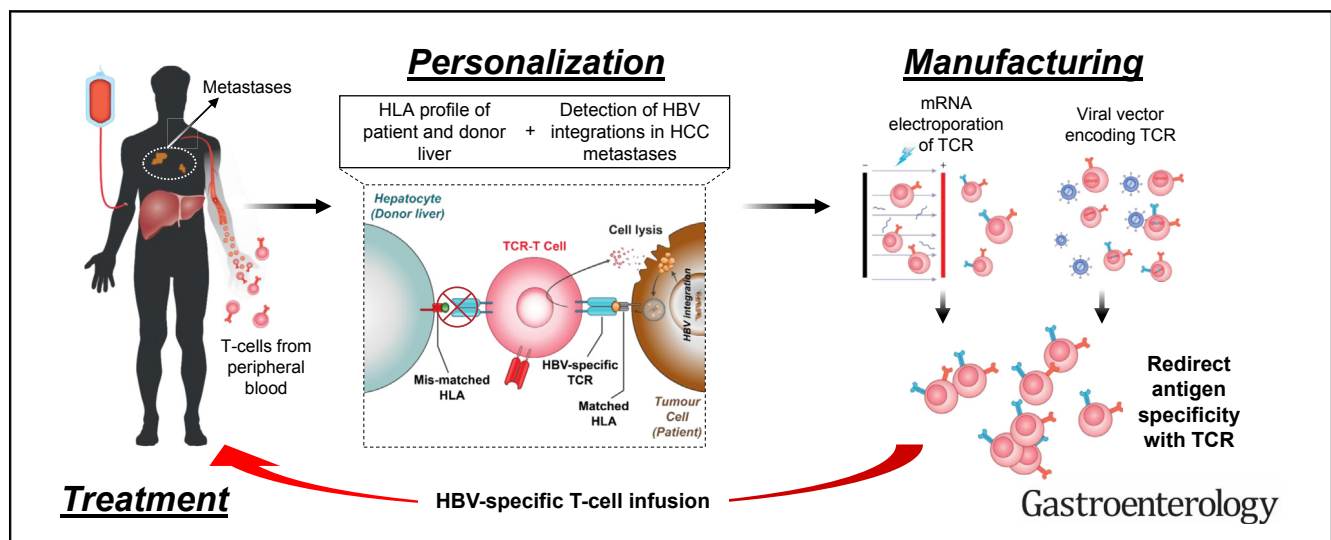




Use of Expression Profiles of HBV-DNA Integrated Into Genomes of Hepatocellular Carcinoma Cells to Select T Cells for Immunotherapy

Anthony Tanoto Tan,^{1,*} Ninghan Yang,^{2,*} Thinesh Lee Krishnamoorthy,^{3,*} Vincent Oei,¹ Alicia Chua,⁴ Xinyuan Zhao,⁴ Hui Si Tan,⁴ Adeline Chia,¹ Nina Le Bert,¹ Diana Low,⁵ Hiang Keat Tan,³ Rajneesh Kumar,³ Farah Gillan Irani,⁶ Zi Zong Ho,⁴ Qi Zhang,⁷ Ernesto Guccione,⁵ Lu-En Wai,^{4,8} Sarene Koh,^{4,8} William Hwang,⁹ Wan Cheng Chow,³ and Antonio Bertoletti^{1,8}

¹Emerging Infectious Diseases, Duke-NUS Medical School, Singapore; ²Genome Institute of Singapore, Agency for Science and Technology (A*STAR), Singapore; ³Department of Gastroenterology and Hepatology, Singapore General Hospital, Singapore; ⁴Lion TCR Pte Ltd, Singapore; ⁵Institute of Molecular and Cell Biology, Agency for Science and Technology (A*STAR), Singapore; ⁶Department of Vascular and Interventional Radiology, Singapore General Hospital, Singapore; ⁷Department of Biotherapy, The Third Affiliated Hospital of Sun Yat-Sen University, Guangdong, China; ⁸Singapore Immunology Network, Agency for Science and Technology (A*STAR), Singapore; ⁹Department of Haematology, Singapore General Hospital, Singapore



BACKGROUND & AIMS: Hepatocellular carcinoma (HCC) is often associated with hepatitis B virus (HBV) infection. Cells of most HBV-related HCCs contain HBV-DNA fragments that do not encode entire HBV antigens. We investigated whether these integrated HBV-DNA fragments encode epitopes that are recognized by T cells and whether their presence in HCCs can be used to select HBV-specific T-cell receptors (TCRs) for immunotherapy. **METHODS:** HCC cells negative for HBV antigens, based on immunohistochemistry, were analyzed for the presence of HBV messenger RNAs (mRNAs) by real-time polymerase chain reaction, sequencing, and Nanostring approaches. We tested the ability of HBV mRNA-positive HCC cells to generate epitopes that are recognized by T cells using HBV-specific T cells and TCR-like antibodies. We then analyzed HBV gene expression profiles of primary HCCs and metastases from 2 patients with HCC recurrence after liver transplantation. Using the HBV-transcript profiles, we selected, from a library of

TCRs previously characterized from patients with self-limited HBV infection, the TCR specific for the HBV epitope encoded by the detected HBV mRNA. Autologous T cells were engineered to express the selected TCRs, through electroporation of mRNA into cells, and these TCR T cells were adoptively transferred to the patients in increasing numbers (1×10^4 – 10×10^6 TCR+ T cells/kg) weekly for 112 days or 1 year. We monitored patients' liver function, serum levels of cytokines, and standard blood parameters. Antitumor efficacy was assessed based on serum levels of alpha fetoprotein and computed tomography of metastases. **RESULTS:** HCC cells that did not express whole HBV antigens contained short HBV mRNAs, which encode epitopes that are recognized by and activate HBV-specific T cells. Autologous T cells engineered to express TCRs specific for epitopes expressed from HBV-DNA in patients' metastases were given to 2 patients without notable adverse events. The cells did not affect liver function over a 1-year period. In 1 patient, 5

of 6 pulmonary metastases decreased in volume during the 1-year period of T-cell administration. **CONCLUSIONS:** HCC cells contain short segments of integrated HBV-DNA that encodes epitopes that are recognized by and activate T cells. HBV transcriptomes of these cells could be used to engineer T cells for personalized immunotherapy. This approach might be used to treat a wider population of patients with HBV-associated HCC.

Keywords: Adoptive T-cell Transfer; TCR; TCR T-cell; HCC.

Hepatocellular carcinoma (HCC), the most common form of liver cancer, is associated with chronic hepatitis B virus (HBV) or hepatitis C virus (HCV) infections.¹ Unlike the RNA-Flavivirus HCV, HBV is a DNA virus that can integrate, as early as 3 days post in vitro infection,² into the chromosome of infected hepatocytes, and more than 90% of HBV-related HCC (HBV-HCC) contains HBV-DNA integrations.³⁻⁵ The potentially curative therapies for HCC are at the moment limited to surgical resection, radiofrequency ablation, and liver transplantation,⁶ whereas systemic therapies provide only a modest increase in overall survival,⁷⁻⁹ so prognosis for these patients remains extremely poor. For this reason, we and others have developed immunotherapeutic approaches in which T cells are redirected with chimeric¹⁰ or classical T-cell receptors (TCRs)^{11,12} able to target HBV antigens/epitopes expressed on normal HBV-infected hepatocytes or in HCC cells. These TCR or chimeric antigen receptor redirected T cells have been shown in animal models to have antiviral¹³ but also anti-HCC efficacy.^{10,12} Furthermore, in a proof-of-concept compassionate treatment of a patient with chronic HBV with post liver transplant recurrence of HBV-HCC,¹⁴ we demonstrated that HCC relapses can be targeted in vivo by T cells engineered with a TCR specific for an HLA-class I restricted epitope derived from whole HBV surface antigen (HBsAg) expressed in the metastases.

The feasibility of such T-cell immunotherapy in this specific patient was because the whole HBsAg was expressed and secreted only by the HCC metastases and not by the transplanted liver. In the absence of detectable HBV replication, the expression of HBsAg was due to the integration of HBV-DNA coding for the whole HBV envelope in the HCC cells. However, unlike in this specific patient, HBV viral integrations do not often encompass the complete open reading frame of HBV antigens. Most of the integrated HBV-DNA are incomplete and the insertion into the human genome results in the generation of HBV-human chimeric proteins.^{15,16} When assayed by antibody-based techniques that depend on recognition of conformational epitopes, HBV-HCC cells with these chimeric proteins would appear negative for HBV antigens, and this explains the fact that HBV-HCC tumors are often indicated as negative for HBV antigens.¹⁷⁻²⁰ As such, the utilization of HBV viral antigens as an HCC-specific tumor antigen has been highly controversial and thought to be only feasible for a small minority of patients with HCC with whole HBV antigens detected.

WHAT YOU NEED TO KNOW

BACKGROUND AND CONTEXT

Most of the HBV-related HCCs contain short HBV-DNA integrations that do not produce whole HBV antigens.

NEW FINDINGS

HCC cells that do not express whole HBV antigens contain short HBV DNA fragments which encode epitopes that can be recognized by and activate T-cells. Analysis of the HBV integrations in liver tumours can guide the appropriate selection of HBV-specific TCR used to engineer T-cells for adoptive immunotherapy of HCC.

LIMITATIONS

The work is an initial proof-of-concept of the approach which will need to be validated in a larger cohort of patients with comprehensive post-treatment follow-up.

IMPACT

A wider population of HCC patients than previously estimated by serological analysis can exploit HBV antigens as tumour-specific targets for T-cell immunotherapy

Here, we first hypothesized that HBV-specific CD8 T-cell epitopes can be derived from short translationally active HBV-DNA integrations present in natural HBV serologically negative HCC cells. This would constitute the rationale of selecting HBV antigens as a robust tumor-associated antigen for HCC, in addition to the demonstration that single-cell genome sequencing of HBV-HCC cells showed remarkable homology of HBV integrations across multiple single tumor cells²¹ despite high overall genetic diversity.^{22,23} Using HBV-specific CD8 T cells and antibody specific for HLA-class I/ HBV epitopes we demonstrated that production and presentation of HBV-specific CD8 T-cell epitopes can take place in naturally HBV serologically negative HCC cells with HBV integration and that their HBV-transcript profile can predict targetability by HBV-specific CD8 T cells. We next used the HBV-transcript profile of HBV-HCC metastases present in 2 patients with HCC relapses after liver transplantation to select the HBV-specific TCRs for personalized TCR T-cell immunotherapy. The functionality of the engineered TCR T cells and their safety and efficacy profile in the treatment of the 2 patients with HBV-related HCC relapses are reported.

*Authors share co-first authorship.

Abbreviations used in this paper: AFP, alpha fetoprotein; bp, base pair; cDNA, complementary DNA; CT, computed tomography; Env/Pol, envelope/polymerase; HBcAg, hepatitis B core antigen; HBsAg, hepatitis B surface antigen; HBV, hepatitis B virus; HBV-HCC, HBV-related HCC; HCC, hepatocellular carcinoma; HCV, hepatitis C virus; IFN, interferon; mRNA, messenger RNA; qPCR, quantitative polymerase chain reaction; TCR, T-cell receptor.

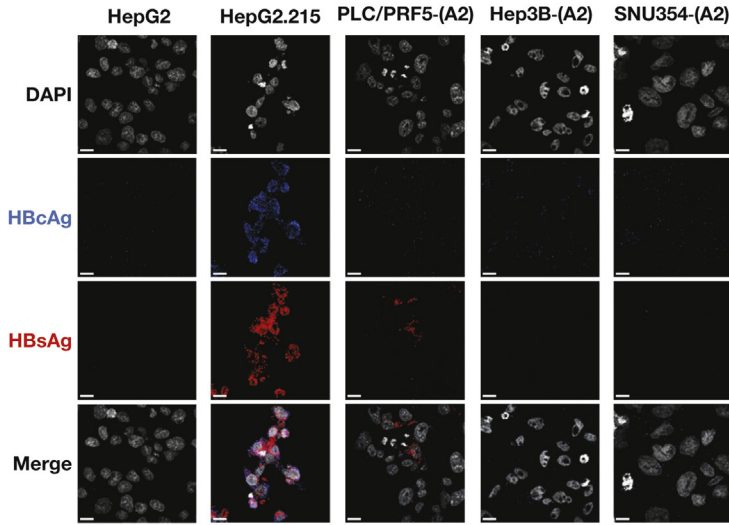
 Most current article

© 2019 by the AGA Institute. Published by Elsevier Inc. This is an open access article under the CC BY-NC-ND license (<http://creativecommons.org/licenses/by-nc-nd/4.0/>).

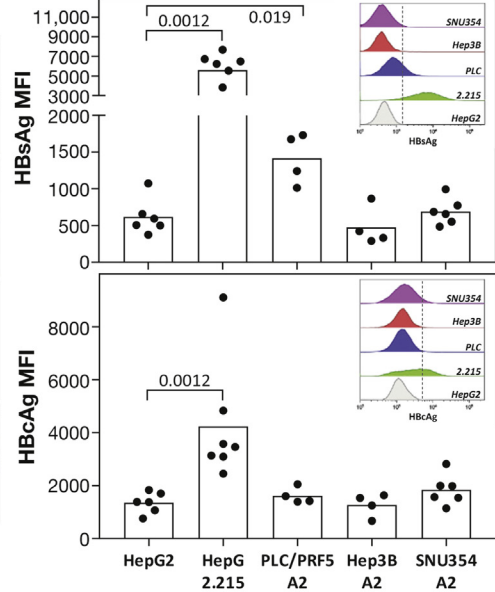
0016-5085

<https://doi.org/10.1053/j.gastro.2019.01.251>

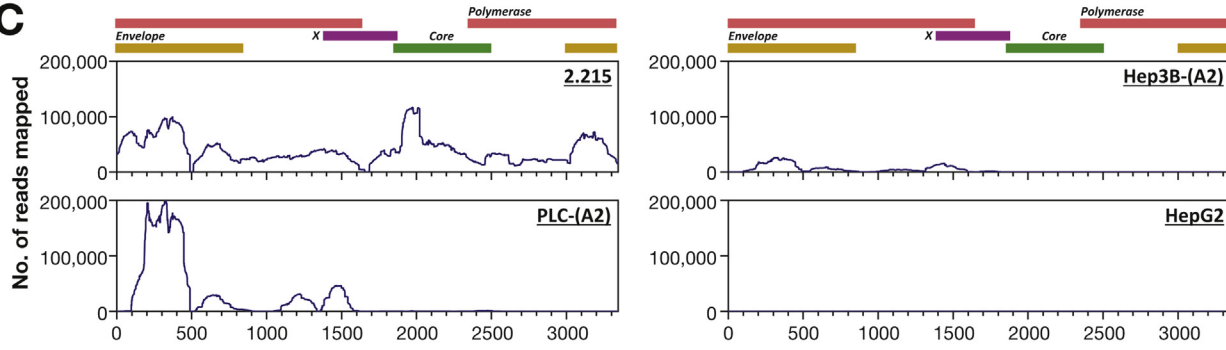
A



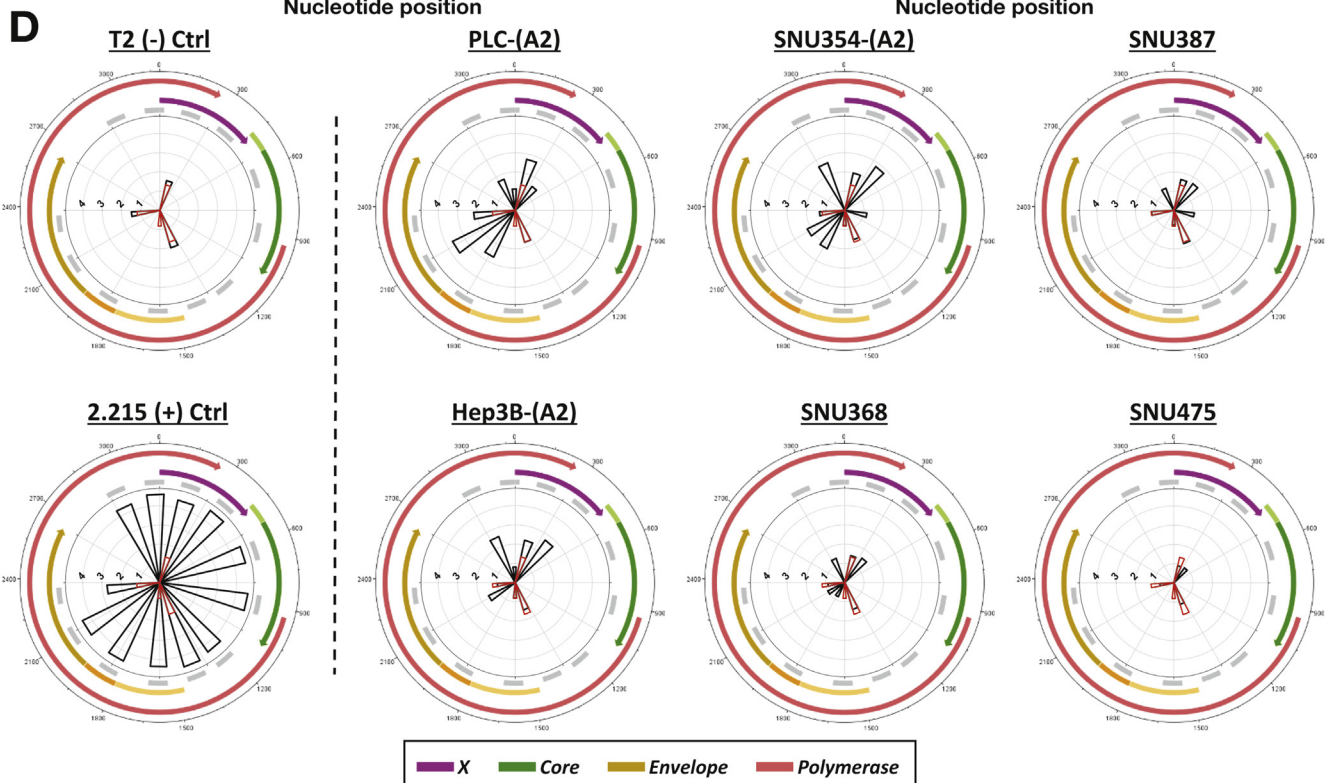
B



C



D



Materials and Methods

Intracellular HBV Antigen Stain by Immunofluorescence Assay

HCC adherent lines were plated on 24-well plate coverslips overnight, washed once with 1x phosphate-buffered saline and fixed with 4% formaldehyde for 20 minutes, followed by permeabilization with 0.1% Triton X-100 for 20 minutes and blocking with 0.2% bovine serum albumin/0.01% Triton X-100 for 1 hour at room temperature. Cells were then incubated with primary antibody of rabbit anti-hepatitis B core antigen (HBcAg) at 1:200 (#7841; Abcam, Cambridge, MA) or mouse anti-HBsAg at 1:300 (#MD050186; Raybiotech, Peachtree Corners, GA) overnight at 4°C, followed by secondary antibodies goat anti-rabbit CF-555 at 1:800 (#SAB4600068; Sigma-Aldrich, St Louis, MO) and goat anti-mouse CF-633 at 1:800 (#SAB4600333; Sigma-Aldrich) for 1 hour at room temperature, before counterstaining with 4',6-diamidino-2-phenylindole (DAPI) at 1:5000. Data acquisition was done using Zeiss (Oberkochen, Germany) LSM710 upright microscope at $\times 40$ and data were analyzed in Zeiss ZEN software.

Sequencing of HBV-specific Transcripts

HBV-specific probes were designed in 50-base pair (bp) regions that were approximately 80 bp apart across the entire HBV genome (genotype D consensus from HBV-DB); 200 ng of ribosomally depleted RNA was used as input for HBV-HCC patient samples, reverse transcribed into complementary DNA (cDNA) and sequencing library prepared according to manufacturer's instructions (NUGEN [Redwood City, CA] Ovation cDNA module for target enrichment # 9103-32, and NUGEN Ovation customized Target Enrichment System #0400-32). cDNA libraries were quantitatively and qualitatively assessed by Bioanalyzer HiSense DNA Chip, followed by 150-bp single end sequencing with Illumina (San Diego, CA) MiSeq.

Reverse-Transcription Quantitative Polymerase Chain Reaction

Quantitative polymerase chain reaction (qPCR) was performed with 2 to 20 ng of reverse-transcribed cDNA per reaction, 0.2–0.7 μM each of forward and reverse primers specific for HBV fragments of interest, and the universal Express SYBR GreenER qPCR supermix (#11784-200; Invitrogen/Life technologies, Carlsbad, CA) or the PowerUp SYBR Green Master Mix (Applied Biosystems, Foster City, CA). β -actin was amplified as an internal control. Cycling conditions were as follows: 95°C for 10 minutes, followed by elongation for 45 cycles at 95°C for 15 seconds, 55°C for 45 seconds or 1 minute, 72°C for 5 seconds.

Melt curve analysis was done to verify the specificity of the reaction. Primer sequences are detailed in the [Supplementary Materials](#).

Nanostring nCounter RNA Quantification

Probesets tiling across the HBV genotype D genome were custom designed by Nanostring (Seattle, WA) based on the consensus sequence of genotype D obtained from the HBV database (<https://hbvdb.ibcp.fr/HBVdb/>); 100 ng of total RNA was used for each analysis and gene expression was quantified using the customized probes and nCounter Standard master kit (NAA-AKIT-048) according to manufacturer's protocol.

xCelligence Real-Time Cytotoxicity Assay

For interferon (IFN)- γ stimulated conditions, 1000 IU/mL of recombinant human IFN- γ was added overnight before being washed 3 times with 1x phosphate-buffered saline. All HCC adherent lines were then trypsinized and seeded in xCELLigence E-Plate VIEW 16 (#06324746001; ACEA Biosciences, San Diego, CA) for 16 to 18 hours and impedance was monitored using the xCELLigence RTCA DP instrument (#00380601050; ACEA Biosciences). CD8+ T cells were then incubated with HCC lines at effector:target 1:1 ratio and impedance was monitored continuously across 3 to 5 days.

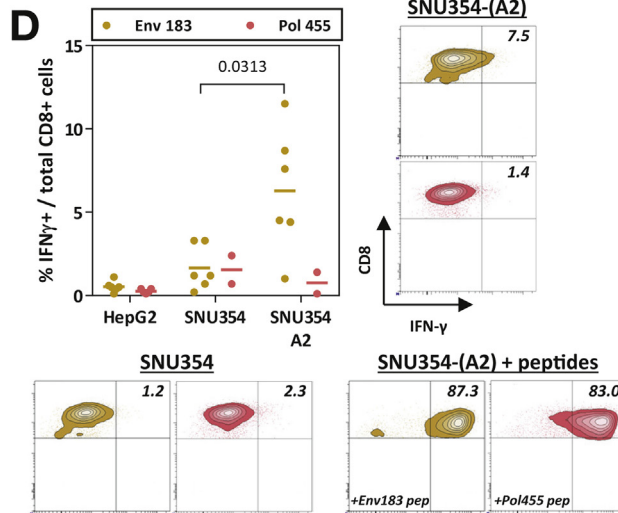
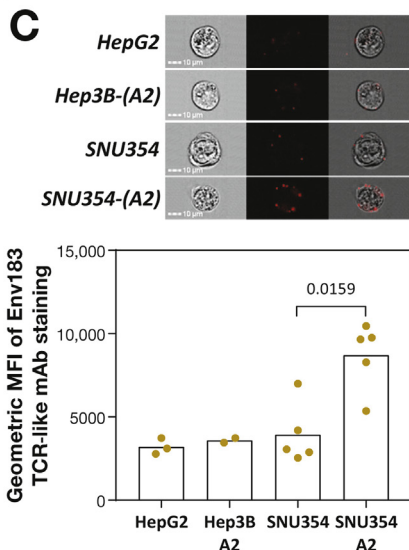
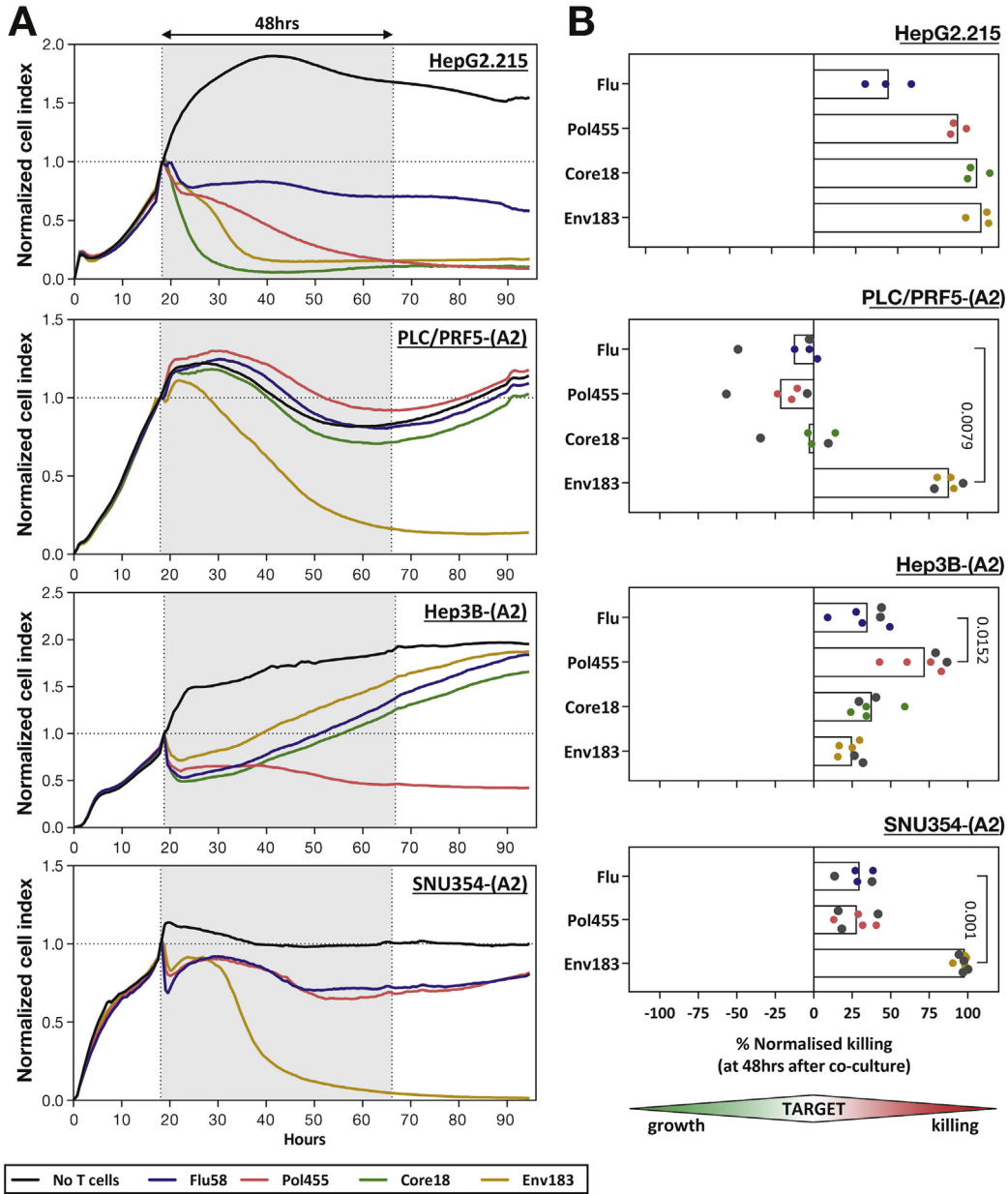
Intracellular HBV Antigen/Cytokine Staining by Flow Cytometry

HCC adherent lines were trypsinized, quenched with media, and followed by live/dead Aqua staining (#L34957; BD Horizon, San Jose, CA). Cells were fixed and permeabilized using BD Cytotfix/Cytoperm (BD Biosciences, San Jose, CA), followed by primary antibody of rabbit anti-HBcAg (#7841; Abcam) or mouse anti-HBsAg (#MD050186; Raybiotech) for 30 minutes on ice, followed by secondary antibodies goat anti-rabbit-CF555 (#SAB4600068; Sigma-Aldrich) and goat anti-mouse-APC (#A865; Life technologies) for 30 minutes on ice. For intracellular cytokine staining, CD8+ T cells were incubated with HCC lines at 1:2 effector to target ratio for 5 hours, followed by live/dead, surface and intracellular stains ([Supplementary Materials and Methods](#)).

HBV-specific T-cell Immunotherapy of Patients With HCC Relapses Post Liver Transplantation

The treatment protocol was approved by the SingHealth Centralised Institutional Review Board of the Singapore General Hospital where the patients were admitted, and informed

Figure 1. HBV-HCC lines negative for HBV antigens can contain fragments of HBV mRNA. (A) Immunofluorescence staining of HBV-HCC lines with HBsAg- (red), HBcAg-specific antibody (blue), and 4',6-diamidino-2-phenylindole (DAPI) (white). The scale bars are 15 μm in length and the images are representative of 2 independent experiments. (B) Quantification of HBsAg and HBcAg expression in HBV-HCC lines by flow cytometry. Bars show the average geometric mean fluorescence intensities (MFI) and each circle denotes a single experiment. A representative experiment is shown in the histogram insert. Significant differences with $P < .05$ are indicated. (C) HBV-transcript profile of HBV-HCC lines obtained from Illumina high-throughput targeted sequencing using probes spanning across the entire HBV genome. Expression levels are shown as the number of reads mapped per nucleotide. (D) HBV-transcript profile of HBV-HCC lines (black) obtained using Nanostring probes covering the HBV genome. Radar plot shows the normalized counts of each HBV-specific probe expressed on a Log_{10} scale. The profile from HepG2 is overlaid in each radar plot (red). The open reading frames of HBV and relative positions of each Nanostring probe are annotated in a similar fashion to [Supplementary Figure 1](#).



consent was obtained from both patients. Detailed clinical history of the patients is found in the [Supplementary Material](#).

Results

HBV mRNA Fragments Are Present in HBV-HCC Cells With Undetectable HBV Antigens

To determine whether specific T-cell recognition of HBV-HCC cells could occur independently of the serological positivity of HBV antigens, we analyzed the expression of HBV antigens in HBV-HCC cell lines. Immunohistochemical visualization ([Figure 1A](#)) and flow cytometric detection ([Figure 1B](#)) of HBsAg and HBcAg confirmed the expression of both antigens in HepG2.215, a cell line constitutively expressing HBV genotype D virus,²⁴ and their absence in the parental HBV-negative HepG2 cells. Recapitulating previous reports, PLC/PRF5-(A2) expresses solely the HBsAg, whereas Hep3B-(A2) and SNU354-(A2) were negative for both HBV antigens tested ([Figure 1A and 1B](#)).^{11,25–27}

We next characterized the HBV-specific transcriptomic profile of the HBV-HCC cell lines by RNA sequencing, by qPCR with HBV-specific primers, and by custom-designed HBV-specific Nanostring assay and compared them with their antigen expression. The relative positions of the primers and Nanostring probes in relation to the open reading frames of HBV are depicted in [Supplementary Figure 1](#). As expected, sequencing reads mapped to the entire HBV genome was detected in HepG2.215, whereas no significant quantities of HBV-specific mRNA were detected in HepG2 ([Figure 1C](#)). In line with the expression of HBsAg detected with antibodies ([Figure 1A and 1B](#)), large quantities of transcripts were mapped to the envelope/polymerase overlapping coding region of the HBV genome in PLC/PRF5-(A2) ([Figure 1C](#)). On the contrary, although HBsAg was not expressed in both Hep3B-(A2) and SNU354-(A2) ([Figure 1A and 1B](#)), HBV-specific mRNA mapping to the envelope/polymerase (Env/Pol) coding region were detected by sequencing, qPCR, and Nanostring ([Figure 1 and Supplementary Figure 2](#)). Thus, using 3 independent detection approaches, we show that HBV-HCC cells can

express short HBV-specific mRNA without antibody detection of HBV antigens.

Translation of HBV mRNA Fragments Generates Functional T-cell Epitopes

Because these short HBV mRNA fragments can result in the formation of HBV/host chimeric proteins,^{15,28} the presence of such transcripts in HBV antigen negative HCC cells might be sufficient to generate functional HBV T-cell epitopes on the cell surface, resulting in their recognition by HBV-specific T cells. We evaluated this possibility using the xCelligence impedance-based cytotoxicity assay.²⁹ HBV mRNA-positive HBV-HCC cell lines were cultured as targets alone, or co-cultured with previously characterized HLA-A2 restricted HBV Core18–27, Env183–191, Pol455–463¹¹ or influenza M1-specific T-cell lines. Nonspecific target lysis was further controlled using the corresponding non-HLA-A2 HBV-HCC cell lines. As expected for HBV-HCC cells with detectable HBV antigens, only the 3 HBV-specific T-cell lines were able to lyse almost all HBV-expressing HepG2.215 cells within 48 hours of co-culture ([Figure 2A and B](#)). Similarly, lysis of HBsAg expressing PLC/PRF5-(A2) was observed only with the Env183–191 T cells ([Figure 2A and B](#)). However, HBV-specific T-cell lines were also able to lyse SNU354-(A2) and Hep3B-(A2) cells ([Figure 2A and B](#)) where only fragments of HBV mRNA were detectable without the presence of the corresponding HBV antigen ([Figure 1](#)). Consistent with the presence of the HBV envelope coding mRNA in SNU354-(A2), only the Env183–191 T cells were able to lyse this target ([Figure 2A and B](#)), whereas lysis of Hep3B-(A2) was instead mediated by the Pol455–463 T cells ([Figure 2A and B](#)). This is not surprising because the HBV Env and Pol coding regions are shared ([Supplementary Figure 1](#)) and the translated protein sequences are discriminated only by the different reading frames. Combined with the random integrations into the host genome, the same fragment of HBV mRNA could be translated to amino acids matching either HBV Env or Pol.

To confirm that the envelope coding transcript positive SNU354-(A2) cells can indeed generate the Env183–91

Figure 2. Functional HBV epitopes are generated by HBV-HCC cells with fragments of HBV mRNA. The ability of HBV-HCC lines to activate epitope-specific T-cell clones were assayed by the xCelligence impedance-based real-time cytotoxicity assay. (A) Representative normalized cell index curves are shown. HBV-HCC lines were cultured for ~18 hours before addition of Core18–27 (green), Env183–191 (brown), Pol455–463 (pink), or Influenza M1 58–66 (blue) T-cell clones. Cell indexes were normalized to the time when T cells were added. (B) Killing of HBV-HCC lines at 48 hours post T-cell addition were summarized. Target killing was normalized to the wells with only HBV-HCC lines cultured (spontaneous target death). Bars show the average normalized killing and each dot represents a single experiment. Gray dots indicate experiments in which 1000 IU/mL of IFN- γ were added in the experiment. Significant differences with $P < .05$ are shown. (C) SNU354-(A2) and SNU354 cell lines were stained with TCR-like antibody specific for the HLA-A0201/Env183–191 complex. Representative brightfield (left column), fluorescent (TCR-like antibody; center column), and merged (right column) images of the respective HBV-HCC cells are shown. Bars show the average geometric MFI of the TCR-like antibody staining for the HBV-HCC lines tested. Each dot represents a single experiment and significant differences with $P < .05$ are indicated. (D) HepG2, SNU354-(A2), and non-HLA-A2 expressing SNU354 were co-cultured with Env183–191 (brown) or Pol455–463 (pink) T-cell clones for 5 hours in the presence of brefeldin-A. SNU354-(A2) was also pulsed with the corresponding HBV peptides before co-culturing with the T-cell clones as a positive control. Representative contour plots are shown and the frequency of IFN- γ + CD8+ cells of total CD8+ T cells are indicated. A summary of these frequencies is shown in the dot plot where the average frequency of IFN- γ + CD8+ cells are indicated and each dot represents a single experiment. Significant differences with $P < .05$ are indicated.

epitope, we first treated the cell line with IFN- γ , a cytokine known to activate intracellular immunoproteasomes and boost HLA-class I presentation. Treatment of SNU354-(A2) cells with IFN- γ (1000 IU/mL) dramatically increased their recognition by Env183–191 T cells. IFN- γ treated SNU354-(A2) cells were completely lysed in less than 6 hours of co-culture in comparison with the approximately 48 hours necessary for the complete killing of untreated SNU354-(A2) cells (Supplementary Figure 3).

Furthermore, we directly analyzed the quantity of Env183–191/HLA-A0201 complexes presented on the surface of SNU354-(A2) cells using a previously developed Env183–191/HLA-A0201 complex specific TCR-like antibody capable of specifically binding the HBV epitope/HLA-class I complexes on HBV-infected hepatocytes.³⁰ From the single-cell images of SNU354-(A2), we observed the presence of the Env183–191/HLA-A0201 complexes on the cell surface, whereas it was absent in both Hep3B-(A2) and non-HLA-A2 expressing SNU354 cells (Figure 2C). Finally, the specific activation of Env183–191 and Pol455–463 T cells by SNU354-(A2) (Figure 2D) and Hep3B-(A2) (Supplementary Figure 4) cells, respectively, was reconfirmed through the flow cytometric detection of intracellular IFN- γ in T cells on co-culture. Hence, we demonstrated that the presence of short HBV mRNA in HCC cells is sufficient to generate functional T-cell epitopes capable of activating HBV-specific T cells.

HBV-HCC Tissues Contain Short HBV mRNA Fragments Without HBsAg or HBcAg Expression

With the demonstration of HBV mRNA+ antigen- HBV-HCC cell line recognition by HBV-specific T cells, we wanted to assess whether fragmented HBV mRNA are indeed expressed in HBV-HCC tissues classified histologically negative for both HBsAg and HBcAg. We analyzed tumor tissues from 20 patients with HBV-HCC by qPCR using the Env/Pol 1 primer pair and with HepG2 and HepG2.215 cells as the negative and positive control, respectively; 15 of 20 HBV-HCC tissues showed detectable quantities of the Env/Pol 1 amplicon (Figure 3A). Although it is not surprising to detect the presence of HBV Env/Pol coding mRNA in the HCC cells of patients with a background of chronic HBV infection, we were also able to detect these mRNA in 8 of 9 HBV-HCC samples that are histologically negative for both HBsAg and HBcAg (Figure 3A; black bars). Using the Nanostring assay, we detected the presence of HBV mRNA from the Env/Pol coding region in 6 of 9 HCC tissues tested, and in these 6 HCC tissues, 4 of them were histologically negative for HBsAg and HBcAg (Figure 3B; red bars). Interestingly, we observed a preferential expression of mRNA from the Pre-S2/S (probes 1–3) and the 3'-polymerase/X (probes 4–7) regions (Figure 3C). This preferential distribution of HBV transcripts would suggest that they were likely generated from HBV integrations and not from episomal HBV-DNA, which should generate mRNA detectable by all the HBV-specific Nanostring probes. Note that because the analyzed HCC tissues were derived from archival samples, experiments of T-cell recognition or TCR-

like antibody staining could not be performed because long-term preservation alters the conformation of HLA-class I epitope complexes.

Profiling of HBV mRNA in Tumor Cells Guides Personalized T-cell Immunotherapy of HBV-HCC

We applied the HBV mRNA profiling approach to determine the suitability of autologous HBV-specific T-cell immunotherapy in 2 patients with HBV-HCC who were diagnosed with HBV-related HCC metastases after liver transplantation. A detailed clinical history is described in the Materials and Methods and schematically represented in Figure 4A and B. Briefly, the 2 patients received allogeneic liver transplantation as a treatment for HBV-related HCC and both patients were serologically negative for HBsAg posttransplant despite the progressive enlargement of the HCC metastases (even with multikinase inhibitor treatment). This differentiates them from the first patient with HCC treated with HBV-specific TCR T cells in whom the whole HBsAg was secreted by the HCC metastases and was detectable in the patient's sera, and in whom HBV epitope/HLA-class I complexes were detected on the HCC.¹⁴ Note that, in these 2 new patients, the biopsy material of the primary HCC and their immunohistology reports did not allow us to define whether the primary HCC lesions were positive for HBV antigens.

The HLA-class I profile of the 2 patients and their respective transplanted livers (shown in Figure 4C and D) indicated that HLA-A0201 and HLA-B5801 restricted TCRs could potentially be used³¹ because they were available in our HBV-TCR library and their mismatch with the HLA-class I haplotype of the transplanted livers would avoid the potential recognition of HBV-infected hepatocytes and thus risk of liver damage.³² We then obtained tumor cells from computed tomography (CT)/ultrasound-guided needle biopsies performed respectively in metastasis located in the retroperitoneum (patient 1) and in the iliac bone (patient 2). Note that the selection of the anatomic locations of the 2 biopsies were based only on their surgical accessibility. The expression profile of mRNA in the envelope and core regions of HBV containing HLA-A0201- (Core18–27 and Env183–191) and HLA-B5801- (LTHB007) restricted T-cell epitopes are shown in Figure 4C and D. The results were compared with the profile obtained in HBV-producing HepG2.215 cells. Different from the HepG2.215, both metastases were negative for core mRNA but expressed envelope mRNA (Figure 4C and D) coding for epitopes that can be recognized by the HLA-A0201- (Env183–191) and HLA-B5801- (LTHB007) TCRs. Interestingly, we were also able to recapitulate the results using archival formalin-fixed, paraffin-embedded sections of the primary HCC of patient 1 (Figure 4C).

This HBV mRNA profile shows that the HCC cells present in both patients are not infected by HBV and/or do not carry full viral DNA, but instead present integrations of HBV-DNA of the Env region (whole or fragmented), which can potentially lead to the generation of HBV T-cell epitopes. Based on the presence of the HBV Env mRNA

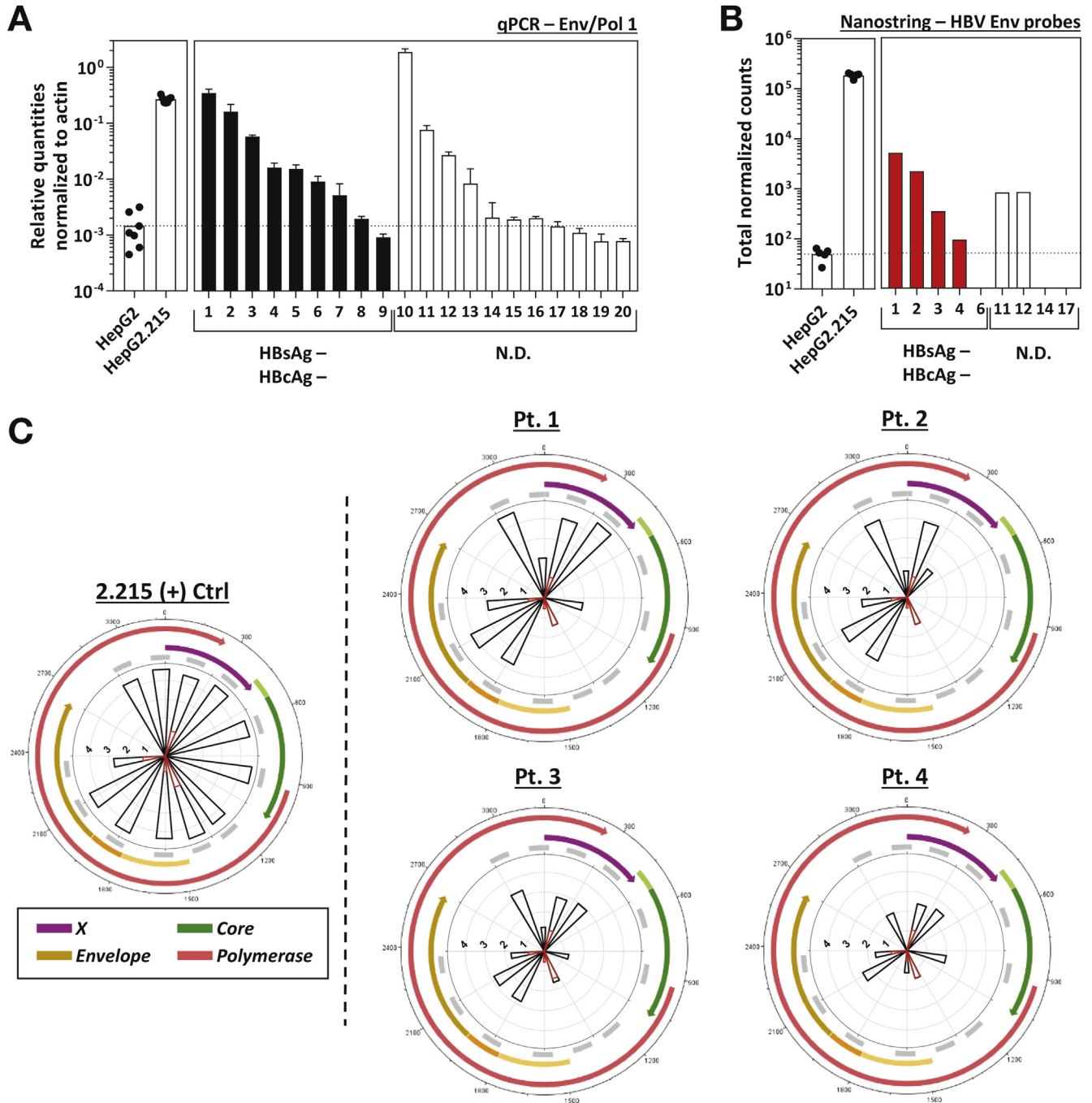


Figure 3. HBV mRNA fragments were found in tumor tissues of patients with HBV-related HCC. HBV envelope-specific mRNA transcripts were quantified in tumor tissues of patients with HBV-related HCC using, (A) qPCR primer pair Env/Pol 1 (n = 20) and (B) HBV-specific Nanostring probes (n = 9). Each analyzed patient is numbered and *solid bars* indicate HCC tissue samples that are HBsAg and HbCag negative by immunohistochemistry. qPCR data were normalized to actin housekeeping controls. Normalized counts of HBV envelope-specific Nanostring probes (probes 1, 2, 3, and 12) were summed and shown in (B). HepG2 and HepG2.215 cells were also analyzed as controls and each *dot* represents a single experiment. (C) HBV-transcript profile of HCC tissues (*black*) obtained using Nanostring probes covering the HBV genome. Radar plots were annotated similar to [Figure 1](#).

transcripts and the discordant HLA-class I molecules of the patient and his donor liver, we selected the HLA-B5801 TCR able to recognize a HBsAg-derived epitope (LTHB007) located in the Env344–377 region for TCR T-cell therapy in both cases.

Production Efficiency of HBV-specific TCR T Cells From Liver-Transplanted Patients Under Immunosuppressive Treatments

The liver is a poorly immunogenic organ. This is why full or partial HLA matching between organ recipient and the

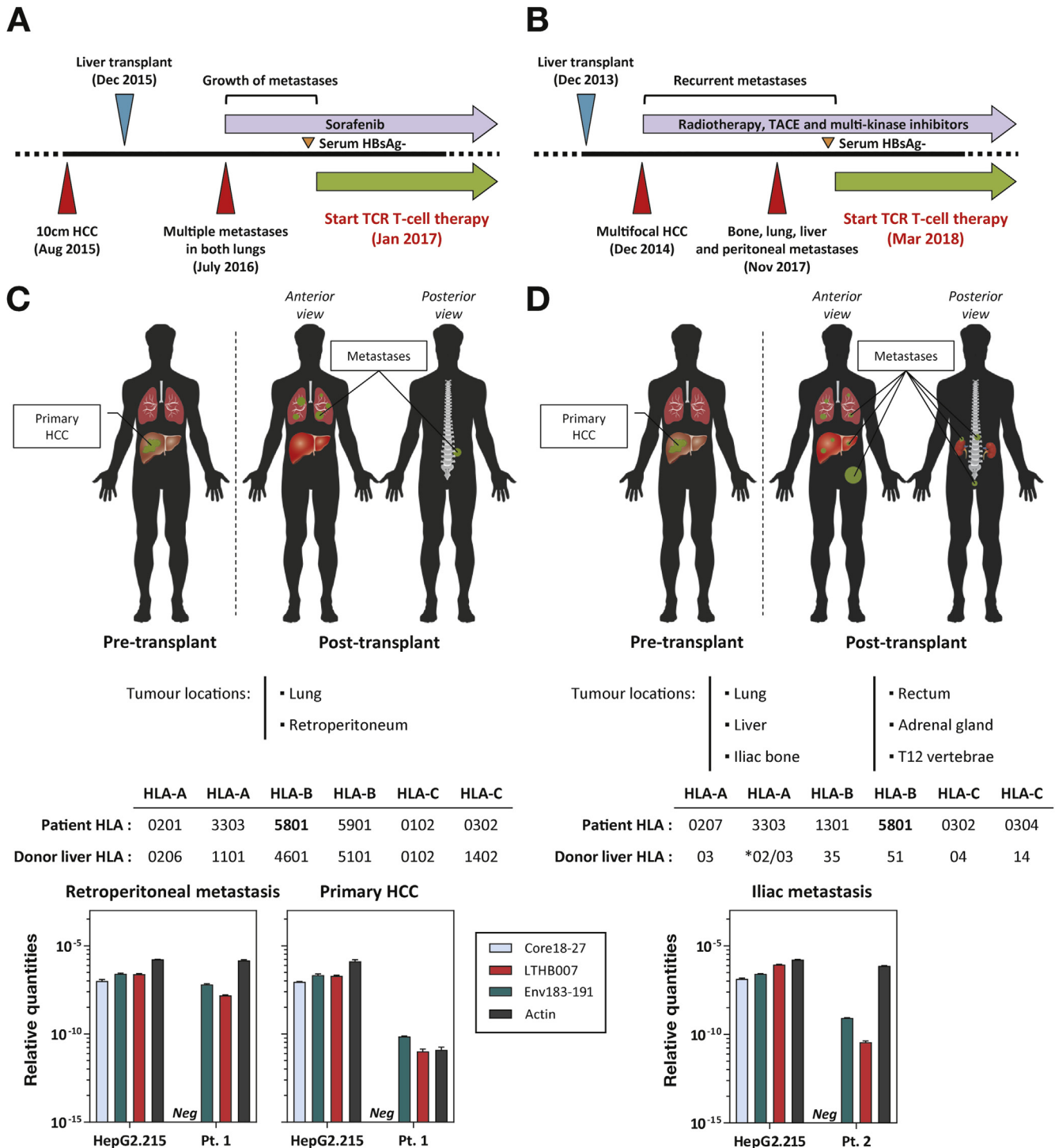


Figure 4. Clinical history of both liver-transplanted HBV-HCC patients treated with autologous HBV-specific TCR T-cells. (A and B) Clinical history of the treated patients indicating the major clinical events and the start of the T-cell immunotherapy. Schematic representation of the primary HCC and metastatic lesions detected posttransplant in patient 1 (C) and patient 2 (D). Anatomic location of the tumor metastases and the HLA-haplotype of both patients and donor livers are listed. The relative quantities of HBV mRNA detected in the tumor tissue obtained from the metastatic nodules and the primary HCC explant were quantified by qPCR using the Core18 and Env/Pol1 primers (Supplementary Materials) and primers specific for the sequence coding the HBV epitope LTHB007. Samples in which no detectable qPCR signals were observed are labeled as “Neg.”

donor is not strictly required for liver transplantation,³³ and why the aim of immunosuppression following liver transplantation has switched from a complete suppression of acute rejection to minimizing the immunosuppression-

related side effects by lowering the drug dose.³⁴ However, because the alloreactive autologous T cells were not negatively selected during development,³⁵ T cells specific for the allogeneic-HLAs of the transplanted livers can be present in

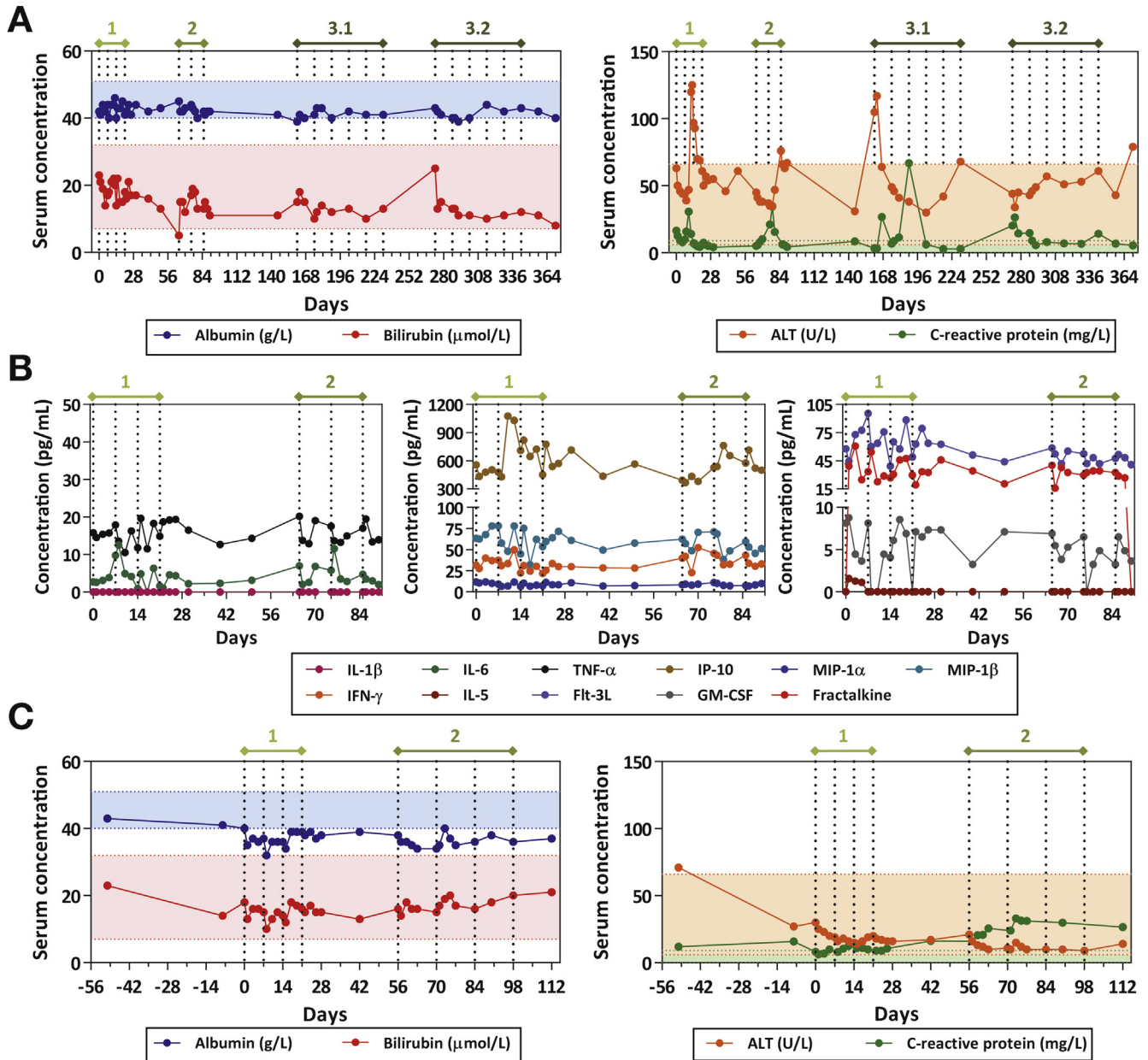
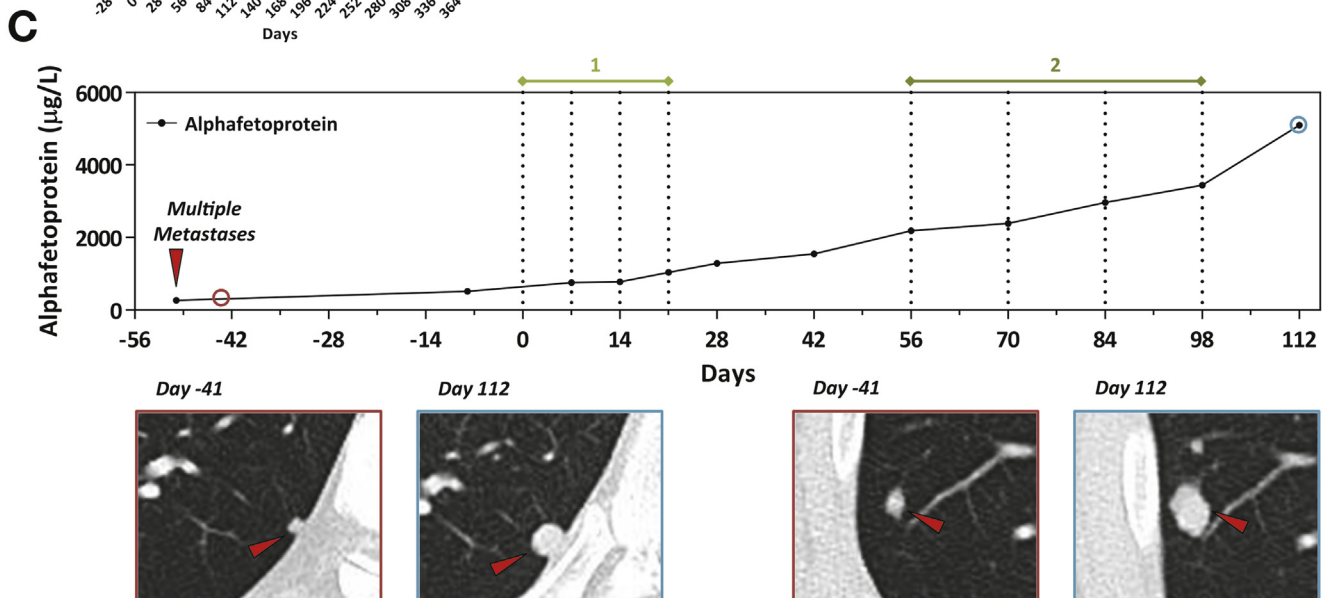
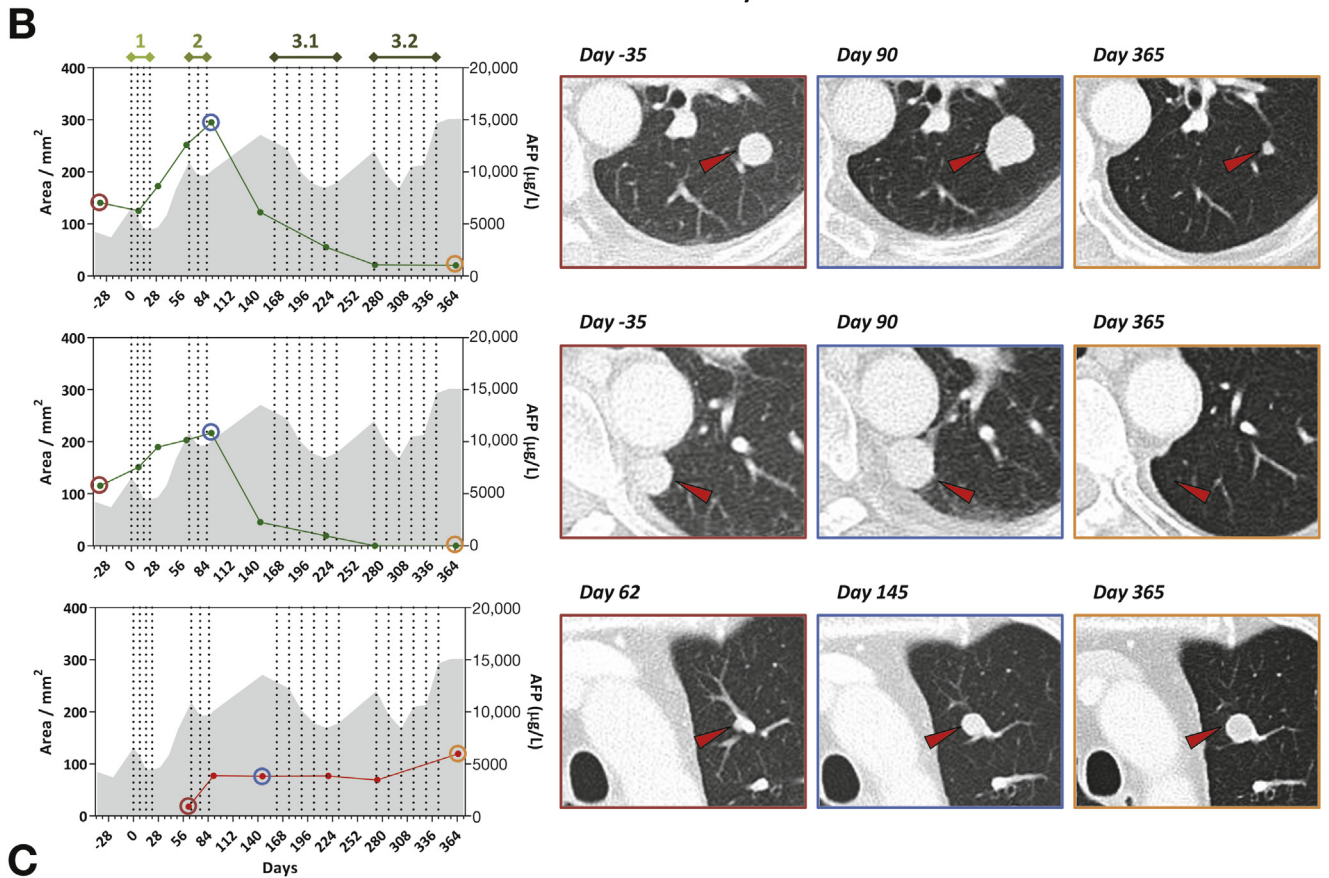
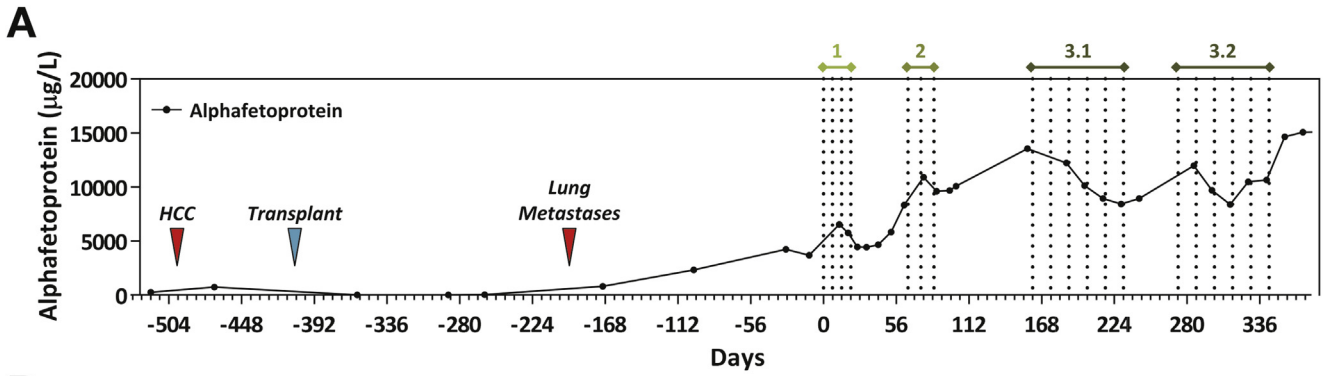


Figure 5. No therapy-related adverse events were observed in both patients treated with HBV-specific TCR T cells. Serum concentrations of albumin (*blue*), bilirubin (*red*), alanine aminotransferase (*orange*), and C-reactive protein (*green*) during the course of the T-cell immunotherapy in patient 1 (A) and patient 2 (C). Day 0 refers to the day of the first infusion. The colored areas represent the reference ranges for each parameter. Vertical dotted lines denote each TCR T-cell infusion and the different phases of the treatment are indicated. (B) Serum concentrations of cytokines, chemokines, and other soluble factors previously associated with severe cytokine release syndrome were analyzed in patient 1. The levels of these analytes were quantified during phases 1 and 2 of the treatment.

the adoptively transferred T cells. Furthermore, growing evidence has shown that allogeneic-HLA reactivity is often mediated by virus-specific TCRs,³⁶ leading to the suggestion that adoptive transfer of virus-specific T cells might mediate transplant rejection.

To reduce the risk of liver graft rejection, we used a simple strategy of adoptively transferring escalating numbers of HBV-specific TCR-redirected T cells that were engineered through mRNA electroporation. This procedure limits the expression of the HBV-specific TCR on activated

T cells to approximately 1 week¹² and allows us to incorporate an initial dose-escalation treatment phase (Phase 1) for added safety (Supplementary Figure 5), which cannot be implemented with TCR T cells produced through stable viral vector transduction. In the absence of clinical signs of liver damage, treatment is continued after 1 month with consecutive doses of 5 to 10 × 10⁶ TCR+ T cells/kg (Phases 2 and 3). The detailed schedule of TCR T-cell infusions in both patients is displayed in Supplementary Figure 5.



Because the treatment requires the production of large numbers of activated T cells for TCR mRNA electroporation, we tested the ability of the T cells of both patients to expand in vitro (Supplementary Figure 6A). Despite the ongoing immunosuppressive treatment, T cells of both patients expanded in vitro (~5-fold expansion) even though it was on average lower than T cells isolated from healthy individuals (Supplementary Figure 6A). TCR expression and the function of the TCR mRNA electroporated T cells engineered for the 2 patients were also monitored. Data from 19 distinct T-cell preparations of patient 1 and from 8 preparations of patient 2 are shown in comparison with data obtained from T cells of 7 different healthy subjects (Supplementary Figure 6B). Despite some variability of TCR expression and IFN- γ production, the data show that we can produce large numbers of functionally active HBV-specific TCR T cells from the peripheral blood mononuclear cells of liver-transplanted patients under immunosuppressive treatments.

Safety of the Autologous HBV-specific TCR T-cell Immunotherapy

We closely monitored the liver function and enzymes throughout the entire course of infusions to determine whether the HBV-TCR T-cell infusion was well tolerated (Figure 5A and C). Note that the data shown have been locked to approximately 1 year of treatment for patient 1 (Phases 1, 2, and 3) and 112 days (Phases 1 and 2) for patient 2 because these are the available data at the time of writing. Both patients are still under treatment at the time of submission of the manuscript. Although alanine aminotransferase levels remain largely unremarkable in both patients, a spike was observed after the third injection (1×10^6 TCR+ T cells/kg) and at the start of phase 3 (10×10^6 TCR+ T cells/kg) in patient 1, but these spikes were concurrent to an episode of deep vein thrombosis and pulmonary embolism event deemed to be unrelated to the TCR T-cell infusions (Figure 5A). Monitoring of C-reactive protein³⁷ and proinflammatory cytokines/chemokine (interleukin-1/interleukin-6)³⁸ levels did not indicate any cytokine release syndrome events (Figure 5). We also examined whether adoptive T-cell transfer triggered a modification of the immune profile. Phenotypic analysis of T cells performed at day 6 and 14 after infusion shows an increase in the frequency of activated (HLA-DR+) and proliferating (Ki67+) CD8 T cells to approximately 10% of total CD8 T cells within 1 week of infusion. These numbers returned to preinfusion levels after 14 days. Whether such modification of the immunological profile was induced on

T-cell infusion or that the adoptively transferred T cells are proliferating in the treated patients remains to be investigated (Supplementary Figure 7).

Last, every CT brain scan performed till date did not detect any intracranial abnormality. All these results show that the therapy is well tolerated and did not pose any significant safety issues in both patients.

Efficacy of the Autologous HBV-specific TCR T-cell Immunotherapy

Finally, we report the assessment of the antitumor efficacy of the treatment through the regular monitoring of the tumor marker alphafetoprotein (AFP) and by CT imaging of the metastatic lesions. In patient 1, both the primary HCC and the posttransplant metastases were overexpressing AFP as evidenced by its elevation at the initial HCC diagnosis, the normalization immediately after liver transplantation, and the reelevation at the time of metastases detection (Figure 6A). On receiving infusions of TCR T cells, serum AFP levels decline and this was consistent across all 4 treatment phases, even for the dose-escalation phase in which doses as low as 10^4 TCR+ T cells/kg were administered (Figure 6A). When infusions were halted during the observation period, AFP levels started to rebound (Figure 6A). This on-therapy decline and off-therapy rebound of AFP levels is expected when mRNA electroporated TCR T cells with transient antitumor function were used.¹² However, such AFP fluctuations were not observed in patient 2 (Figure 6C). To gather direct evidence of the antitumor effects, we quantified the maximum cross-sectional area of the metastatic lesions (patient 1: 6 pulmonary lesions and 1 retroperitoneal lesion; patient 2: 2 pulmonary lesions) using the CT images obtained at regular intervals (Figure 6B and C and Supplementary Figure 8). Five of 6 pulmonary lesions in patient 1 decreased in size while the last pulmonary and retroperitoneal metastasis remained largely stable (Figure 6B and Supplementary Figure 8). One of the pulmonary lesions (Figure 6B, middle row) has completely disappeared without recurrence till date. Interestingly, reduction of tumor size occurred only between 5 and 60 days after the seventh infusion (Figure 6B and Supplementary Figure 8A), at a period in which mRNA electroporated TCR T cells would have little or no expression of the introduced HBV-specific TCR. On the other hand, the metastatic lesions present in patient 2 (Figure 6C) showed instead a robust enlargement 20 days after infusion of the last TCR T-cell dose. However, because reduction in tumor size occurred only approximately 90 to 140 days after therapy initiation for patient 1, the antitumor effects

Figure 6. Monitoring of treatment response in both TCR T-cell-treated patients. Serum concentrations of AFP in patient 1 (A) and patient 2 (C) from before treatment until the end of the indicated treatment phases are shown. Vertical dotted lines denote each TCR T-cell infusion and the different phases of the treatment are indicated. (B) The largest cross-sectional area of all tumor nodules detected in the lungs of patient 1 (Supplementary Figure 8) were measured at specific intervals during the therapy and 3 representative nodules are shown. Gray-shaded areas represent the serum AFP concentrations. CT images of the corresponding tumor nodules at 3 indicated time points (red, blue, and orange) are shown and the lesions are indicated by the red arrow. (C) CT images of 2 representative tumor nodules in the lungs of patient 2 at the indicated time points (red and cyan) are shown and the lesions are indicated by the red arrow.

that could be present for patient 2 are too early to be determined.

Discussion

We previously used HBV-TCR-redirected T cells in a patient who presented HBsAg+ HCC relapses after liver transplantation,¹⁴ demonstrating that HBV antigens can indeed function as tumor-associated antigens. However, the use of HBV proteins as tumor antigens for HCC immunotherapy has been criticized because of their frequent lack of expression in HCC.^{17–20}

In this work, we wanted to challenge this concept because of the inherent differences between classical antibody-based assays used in clinics to detect HBV antigens and T-cell recognition of HBV-HCC cells through TCR and HLA/epitope complex interactions. Although the former recognizes the conformationally intact HBV antigens per se, T-cell recognition of HCC cells requires only the presentation of an internally processed epitope complexed with the appropriate HLA-class I molecules. These epitopes could potentially be derived from short translationally active HBV integrations that are known to be commonly present in HBV-HCC. Thus, the absence of antibody-detectable HBV antigens in HBV-HCC cells should not exclude them from being targeted by HBV-specific T cells. This was demonstrated by comparing the antigen expression with the presence of HBV-specific mRNA in HBV-HCC cell lines in vitro and in archived HBV-HCC tissues from patients, and by showing that HBV-specific T-cell recognition of HBV-HCC cells could occur in the presence of short HBV-specific mRNA independent of the antibody detection of HBV antigens. These data imply that HBV mRNA expression profile can predict, with greater accuracy than HBV protein detection by antibodies, the potential generation of HBV epitopes recognized by HBV-specific TCR in HCC.

Important clinical implications can be derived by the experimental evidence that HBV antigen negative but HBV mRNA-positive HCC can be recognized by HBV-specific TCRs. First, because the analysis of HBV-specific mRNA transcripts in HCC cells can be performed in both fresh biopsy material or in archived tissues that are unsuitable for immunohistological analysis of whole HBV antigen expression, it facilitates the evaluation of potential candidates for HCC T-cell therapy. Second, as shown in this work, it allows us to test the suitability of HBV serologically negative liver-transplanted patients with relapses of HBV-related HCC for HBV-specific TCR T-cell immunotherapy. However, other categories of patients with HCC might also benefit from T-cell therapies relying on HBV epitopes derived from short integrated HBV-DNA fragments. Frequent HBV-DNA integrations due to occult HBV infection have been detected in a large proportion of HCCs occurring in HBV serologically negative patients with HCV chronic hepatitis and even alcoholic hepatitis.³⁹ Theoretically, the detection of HBV-specific mRNA in the tumors of patients with HCC diagnosed with non-HBV-related etiologies, might allow the inclusion of these patients for possible HCC immunotherapy with HBV-TCR-redirected T cells. The low frequency of

HBV-infected nonmalignant hepatocytes in the occult HBV patients might also allow the treatment of patients with primary HCC without an overt risk of on-target off-tumor effects.

The treatment of HCC in these “occult HBV” patients is still a hypothesis, but we had the opportunity to directly test the translational utility of our in vitro findings in 2 patients who were chronically infected with HBV before liver transplantation but remain HBV serologically negative despite the development of HCC relapses. We used the information obtained by the HBV mRNA profile present in their metastasis to select the appropriate HBV-specific TCR for their personalized immunotherapy treatment. We detected a significant volume reduction of several pulmonary HCC metastases, linked with a temporal drop of AFP after TCR T-cell infusion in 1 of the 2 patients. These data suggest that the T cells engineered with the selected HBV-TCR do recognize in vivo the HCC relapses, a finding that indirectly supports the rationale of using the HBV mRNA transcript profile present in HCC cells for the appropriate selection and personalization of patients with HCC and the related T-cell immunotherapy, respectively. Instead, we could not observe any clear signs of therapy efficacy in the second treated patient, even though the robust volumetric expansion (pseudo progression) of the lesion observed after the second cycle of TCR therapy (day 112) was similar to the volumetric changes observed in patient 1. This expansion was, however, not followed by any volumetric reduction of the lung metastases of patient 2. It is clear that treatment efficacy cannot be evaluated in only 2 subjects. However, this initial trial of escalating doses of mRNA electroporated HBV-specific TCR T cells provided several important indications. First, we demonstrated that it is possible to expand and produce HBV-TCR-redirected T cells using peripheral blood mononuclear cells isolated from liver-transplanted patients under immunosuppressive treatment. Preliminary data also showed an elevation of the frequency of activated and proliferating CD8 T cells in the peripheral blood of patient 1 within a week of TCR T-cell infusion (Supplementary Figure 7), indicating that activation and proliferation could occur even in the presence of immunosuppression. We also showed that the adoptive transfer of HBV-specific TCR T cells exhibited excellent safety with no treatment-related adverse events observed throughout the course of 19 infusions in patient 1 and 8 infusions in patient 2, supporting further deployment of T-cell-based immunotherapy in liver-transplanted patients.

Interestingly, the observed reduction pattern of the size of the pulmonary metastases in patient 1 is peculiar, because in an HBV-HCC mouse model, the adoptive transfer of mRNA electroporated TCR T cells exerted only a transient antitumor effect.¹² Here, not only is the reduction of the size of almost all pulmonary lesions (Figure 6B and Supplementary Figure 8A) durable, it was observed during the second observation period, between 5 and 60 days after the last infusion (seventh infusion). Taken together with the transient HBV-specific TCR expression of the TCR T cells, it is unlikely that the tumor regression was solely mediated by the cytotoxic activity of the adoptively transferred T cells.

Instead, the data suggest that the HBV-specific TCR T-cell infusions might have induced a secondary tumor-specific immune response that mediated the reduction of the metastases, a concept frequently described in the cancer-immunity cycle.⁴⁰

In conclusion, we think that the data present in this work supports the rationale of considering HBV antigens as a specific tumor antigen for T-cell immunotherapy in all the patients with HCC in whom integration of fragments of translationally active HBV-DNA are the only evidence of HBV involvement. These results, together with the safety profile offered by the utilization of T cells transiently expressing TCR through mRNA electroporation in liver transplant patients will allow us to properly analyze in a large patient population, the clinical efficacy and mechanisms of action of HBV-specific TCR T cells that have been at the moment only relegated to the treatment of few selected cases of HCC.

Supplementary Material

Note: To access the supplementary material accompanying this article, visit the online version of *Gastroenterology* at www.gastrojournal.org, and at <https://doi.org/10.1053/j.gastro.2019.01.251>.

References

1. Global Burden of Disease Liver Cancer Collaboration, Akinyemiju T, Abera S, et al. The Burden of Primary Liver Cancer and Underlying Etiologies From 1990 to 2015 at the Global, Regional, and National Level: Results From the Global Burden of Disease Study 2015. *JAMA Oncol* 2017;3:1683–1691.
2. Tu T, Budzinska MA, Vondran FWR, et al. Hepatitis B virus DNA integration occurs early in the viral life cycle in an in vitro infection model via NTCP-dependent uptake of enveloped virus particles [published online ahead of print February 7, 2018]. *J Virol* <https://doi.org/10.1128/JVI.02007-17>
3. Amaddeo G, Cao Q, Ladeiro Y, et al. Integration of tumour and viral genomic characterizations in HBV-related hepatocellular carcinomas. *Gut* 2015;64:820–829.
4. Sung WK, Zheng H, Li S, et al. Genome-wide survey of recurrent HBV integration in hepatocellular carcinoma. *Nat Genet* 2012;44:765–769.
5. Tang KW, Alaei-Mahabadi B, Samuelsson T, et al. The landscape of viral expression and host gene fusion and adaptation in human cancer. *Nat Commun* 2013;4:2513.
6. Raza A, Sood GK. Hepatocellular carcinoma review: current treatment, and evidence-based medicine. *World J Gastroenterol* 2014;20:4115–4127.
7. El-Khoueiry AB, Sangro B, Yau T, et al. Nivolumab in patients with advanced hepatocellular carcinoma (CheckMate 040): an open-label, non-comparative, phase 1/2 dose escalation and expansion trial. *Lancet* 2017;389:2492–2502.
8. Llovet JM, Ricci S, Mazzaferro V, et al. Sorafenib in advanced hepatocellular carcinoma. *N Engl J Med* 2008;359:378–390.
9. Bruix J, Qin S, Merle P, et al. Regorafenib for patients with hepatocellular carcinoma who progressed on sorafenib treatment (RESORCE): a randomised, double-blind, placebo-controlled, phase 3 trial. *Lancet* 2017;389:56–66.
10. Krebs K, Bottinger N, Huang LR, et al. T cells expressing a chimeric antigen receptor that binds hepatitis B virus envelope proteins control virus replication in mice. *Gastroenterology* 2013;145:456–465.
11. Gehring AJ, Xue SA, Ho ZZ, et al. Engineering virus-specific T cells that target HBV infected hepatocytes and hepatocellular carcinoma cell lines. *J Hepatol* 2011;55:103–110.
12. Koh S, Shimasaki N, Suwanarusk R, et al. A practical approach to immunotherapy of hepatocellular carcinoma using T cells redirected against hepatitis B virus. *Mol Ther Nucleic Acids* 2013;2:e114.
13. Kah J, Koh S, Volz T, et al. Lymphocytes transiently expressing virus-specific T cell receptors reduce hepatitis B virus infection. *J Clin Invest* 2017;127:3177–3188.
14. Qasim W, Brunetto M, Gehring AJ, et al. Immunotherapy of HCC metastases with autologous T cell receptor redirected T cells, targeting HBsAg in a liver transplant patient. *J Hepatol* 2015;62:486–491.
15. Chiu YT, Wong JK, Choi SW, et al. Novel pre-mRNA splicing of intronically integrated HBV generates oncogenic chimera in hepatocellular carcinoma. *J Hepatol* 2016;64:1256–1264.
16. Furuta M, Tanaka H, Shiraishi Y, et al. Characterization of HBV integration patterns and timing in liver cancer and HBV-infected livers. *Oncotarget* 2018;9:25075–25088.
17. Wang Y, Wu MC, Sham JS, et al. Different expression of hepatitis B surface antigen between hepatocellular carcinoma and its surrounding liver tissue, studied using a tissue microarray. *J Pathol* 2002;197:610–616.
18. Melis M, Diaz G, Kleiner DE, et al. Viral expression and molecular profiling in liver tissue versus microdissected hepatocytes in hepatitis B virus-associated hepatocellular carcinoma. *J Transl Med* 2014;12:230.
19. Yen CJ, Ai YL, Tsai HW, et al. Hepatitis B virus surface gene pre-S2 mutant as a high-risk serum marker for hepatoma recurrence after curative hepatic resection. *Hepatology* 2018;68:815–826.
20. Fu S, Li N, Zhou PC, et al. Detection of HBV DNA and antigens in HBsAg-positive patients with primary hepatocellular carcinoma. *Clin Res Hepatol Gastroenterol* 2017;41:415–423.
21. Duan M, Hao J, Cui S, et al. Diverse modes of clonal evolution in HBV-related hepatocellular carcinoma revealed by single-cell genome sequencing. *Cell Res* 2018;28:359–373.
22. Hou Y, Guo H, Cao C, et al. Single-cell triple omics sequencing reveals genetic, epigenetic, and transcriptomic heterogeneity in hepatocellular carcinomas. *Cell Res* 2016;26:304–319.
23. Ling S, Hu Z, Yang Z, et al. Extremely high genetic diversity in a single tumor points to prevalence of non-

- Darwinian cell evolution. *Proc Natl Acad Sci U S A* 2015; 112:E6496–E6505.
24. Acs G, Sells MA, Purcell RH, et al. Hepatitis B virus produced by transfected Hep G2 cells causes hepatitis in chimpanzees. *Proc Natl Acad Sci U S A* 1987;84:4641–4644.
 25. Park JG, Lee JH, Kang MS, et al. Characterization of cell lines established from human hepatocellular carcinoma. *Int J Cancer* 1995;62:276–282.
 26. MacNab GM, Alexander JJ, Lecatsas G, et al. Hepatitis B surface antigen produced by a human hepatoma cell line. *Br J Cancer* 1976;34:509–515.
 27. Twist EM, Clark HF, Aden DP, et al. Integration pattern of hepatitis B virus DNA sequences in human hepatoma cell lines. *J Virol* 1981;37:239–243.
 28. **Wooddell CI, Yuen MF**, Chan HL, et al. RNAi-based treatment of chronically infected patients and chimpanzees reveals that integrated hepatitis B virus DNA is a source of HBsAg. *Sci Transl Med* 2017;9. <https://doi.org/10.1126/scitranslmed.aan0241>.
 29. Peper JK, Schuster H, Loffler MW, et al. An impedance-based cytotoxicity assay for real-time and label-free assessment of T-cell-mediated killing of adherent cells. *J Immunol Methods* 2014;405:192–198.
 30. Sastry KS, Too CT, Kaur K, et al. Targeting hepatitis B virus-infected cells with a T-cell receptor-like antibody. *J Virol* 2011;85:1935–1942.
 31. Banu N, Chia A, Ho ZZ, et al. Building and optimizing a virus-specific T cell receptor library for targeted immunotherapy in viral infections. *Sci Rep* 2014;4:4166.
 32. Bertoletti A, Brunetto M, Maini MK, et al. T cell receptor-therapy in HBV-related hepatocellular carcinoma. *Oncoimmunology* 2015;4:e1008354.
 33. Navarro V, Herrine S, Katopes C, et al. The effect of HLA class I (A and B) and class II (DR) compatibility on liver transplantation outcomes: an analysis of the OPTN database. *Liver Transpl* 2006;12:652–658.
 34. European Association for the Study of the Liver. EASL clinical practice guidelines: liver transplantation. *J Hepatol* 2016;64:433–485.
 35. Sherman LA, Chattopadhyay S. The molecular basis of allorecognition. *Annu Rev Immunol* 1993;11:385–402.
 36. Amir AL, D’Orsogna LJ, Roelen DL, et al. Allo-HLA reactivity of virus-specific memory T cells is common. *Blood* 2010;115:3146–3157.
 37. Davila ML, Riviere I, Wang X, et al. Efficacy and toxicity management of 19–28z CAR T cell therapy in B cell acute lymphoblastic leukemia. *Sci Transl Med* 2014; 6:224ra25.
 38. Norelli M, Camisa B, Barbiera G, et al. Monocyte-derived IL-1 and IL-6 are differentially required for cytokine-release syndrome and neurotoxicity due to CAR T cells. *Nat Med* 2018;24:739–748.
 39. Saitta C, Tripodi G, Barbera A, et al. Hepatitis B virus (HBV) DNA integration in patients with occult HBV infection and hepatocellular carcinoma. *Liver Int* 2015;35:2311–2317.
 40. Chen DS, Mellman I. Oncology meets immunology: the cancer-immunity cycle. *Immunity* 2013;39:1–10.

Author names in bold designate shared co-first authorship.

Received October 23, 2018. Accepted January 17, 2019.

Reprint requests

Address requests for reprints to: Antonio Bertoletti, MD, Emerging Infectious Diseases Programme, DUKE-NUS Medical School, 8 College Road, Singapore 169857, Singapore. e-mail: antonio@duke-nus.edu.sg.

Acknowledgments

We acknowledge Frances Jin and Alvin Tan of Lion TCR Pte. Ltd. for their help in the production of functional mRNA used in the immunotherapy of both patients described in this work. We also thank Dr Evan Newell and Ms Karen Teng for their help in the CyTOF analysis of the patient peripheral blood mononuclear cells.

Author Contributions: ATT, NY, EG, SK, LW, and AB designed the study. ATT, NY, and AB drafted the manuscript. ATT, NY, VO, NLB, AC, ZX, DL, AC, THS, and HZZ performed the experiments. ATT, NY, DL, NLB, and LW analyzed and interpret the data. QZ provided clinical material. TLK, HKT, RK, FGI, WH, and WCC provided clinical care for the patients and all clinical data.

Conflicts of interest

These authors disclose the following: Antonio Bertoletti participates in advisory boards on hepatitis B virus immune therapy for Gilead, Janssen, Springbank, Vir, Abivax, and Jiangsu Simcere Pharmaceutical. Antonio Bertoletti and Anthony Tanoto Tan are also the Scientific Founder and the Scientific Consultant of Lion TCR Pte. Ltd., respectively. The remaining authors disclose no conflicts.

Funding

This research is supported by the Singapore Ministry of Health’s National Medical Research Council under its Singapore Translational Research Investigator Award (MOH-STaR17nov-0001).

Supplementary Material and Methods

Cell Culture Maintenance

HepG2 cells were cultured in Dulbecco's modified Eagle's medium (DMEM) supplemented with 10% heat-inactivated fetal bovine serum, 100 IU/mL penicillin, 100 μ g/mL streptomycin, and Glutamax (Invitrogen, Carlsbad, CA). HepG2.2.15 cells were cultured in DMEM supplemented as described previously with additional minimum essential medium nonessential amino acids (Invitrogen), sodium pyruvate (Invitrogen), and selected using 150 μ g/mL of G418 (Sigma-Aldrich, St. Louis, MO).

T2, Epstein-Barr virus (EBV) B cells, PLC/PRF5, PLC/PRF5-(A2) (transduced with HLA-A0201), SNU354, SNU354-(A2) (transduced with HLA-A0201), and SNU cell lines (SNU368, SNU387, SNU398, SNU475) were maintained in RPMI 1640 supplemented with 10% heat-inactivated fetal bovine serum, 20 mM HEPES, 0.5 mM sodium pyruvate, 100 IU/mL penicillin, 100 μ g/mL streptomycin, minimum essential medium essential and nonessential amino acids (Invitrogen), and Glutamax. Hep3B and Hep3B-(A2) (transduced with HLA-A0201) were maintained in DMEM supplemented as described previously.

Cell lines that were transduced with HLA-A0201 were selected with 2 μ g/mL puromycin. For the IFN- γ treatment conditions, hepatocellular carcinoma lines with HBV DNA integration were treated with IFN- γ (R&D systems, Minneapolis, MN) at 1000 IU/mL for 16 to 24 hours prior.

RNA Isolation

A total of 500,000 cells were harvested from the HCC cell lines, and total RNA was isolated using the Qiagen RNAeasy Micro Kit with DNase treatment, according to the manufacturer's instructions (#74004; Qiagen). The quantity and quality of RNA was assessed by Nanodrop (Thermo Scientific). Tissue samples from HBV-HCC patient samples were either stored at -80°C in RNAlater or as formalin-fixed paraffin-embedded (FFPE) tissue. Total RNA was isolated from FFPE tissue using the AllPrep DNA/RNA FFPE kit (Qiagen) according to the manufacturer's instructions. For tissue samples stored in RNA later, tissue sections were sliced and harvested using Tissuelyser LT, followed by RNA extraction using the Qiagen RNAeasy Micro Kit with DNase treatment according to the manufacturer's instructions. RNA concentration was determined using a Nanodrop, and a minimum of 50 ng was reverse transcribed using the iScript Select cDNA Synthesis Kit (Bio-Rad).

qPCR Primer Sequences

β -actin forward: 5'-CACCATTGGCAATGAGCGGTTTC-3'
 β -actin reverse: 5'-AGGTCTTTGCGGATGTCCACGT-3'
 Core forward: 5'-GGCATGGACATTGACCCTTA-3'
 Core reverse: 5'-CACCCACCCAGGTAGCTAGA-3'
 Env/Pol 1 forward: 5'-TAGGACCCCTGCTCGTGTTA-3'
 Env/Pol 1 reverse: 5'-CCCCTAGAAAATTGAGA-GAAGTCCA-3'
 Env/Pol 2 forward: 5'-ATCCTGCTGCTATGCCTCAT-3'

Env/Pol 2 reverse: 5'-GTCCGAAGGTTTGGTACAGC-3'
 Core18 forward: 5'-AAGAATTTGGAGCTACTGTGGA-3'
 Core18 reverse: 5'-TTCCCGATACAGAGCTGAGG-3'
 LTHB007 forward: 5'-CAGTGGTTCGTAGGGCTTTC-3'
 LTHB007 reverse: 5'-GCGGTAAAAAGGGACTCAAG-3'

Bioinformatic Analysis of HBV-specific High-Throughput Sequencing

Illumina sequenced reads were first adapter-trimmed using cutadapt (parameters: -minimum-length 50 -q 10 -overlap 25 -no-indels). Potential human ribosomal RNA reads were removed using bowtie2 with default parameters. Reads were then aligned both to the human genome (hg19) and the HBV genome using STAR v2.4.2a (parameters: -twopassMode Basic -chimSegmentMin 15 -alignSJD-BoverhangMin 10 -alignMatesGapMax 200000 -alignIntronMax 200000 -chimOutType SeparateSAMold -outSAMstrandField intronMotif). Pileup read counts for reads aligning to the HBV genome were generated with samtools mpileup.

Intracellular HBV Antigen/Cytokine Staining by Flow Cytometry

HCC adherent lines were trypsinized, quenched with media, and followed by live/dead Aqua staining (#L34957; BD Horizon). Cells were fixed and permeabilized using BD Cytofix/Cytoperm (BD Biosciences), followed by primary antibody of rabbit anti-HBcAg (#7841; Abcam) or mouse anti-HBsAg (#MD050186; Raybiotech) for 30 minutes on ice, followed by secondary antibodies goat anti-rabbit -CF555 (#SAB4600068; Sigma-Aldrich) and goat anti-mouse APC (#A865; Life technologies) for 30 minutes on ice.

For intracellular cytokine staining, CD8+ T cells were incubated with HCC lines at 1:2 effector to target ratio in the presence of CD107a-FITC (#555800; BD Pharmingen, San Jose, CA) for 5 hours, followed by live/dead NIR (#L10119; Invitrogen) staining and by surface staining for CD8-V500 (#560774; BD Horizon). T cells were then fixed and permeabilized using BD Cytofix/Cytoperm (BD Biosciences) and subjected to intracellular cytokine staining using TNF-PE (#559321; BD Pharmingen) and IFN- γ -PE-Cy7 (#25-7319-82; eBioscience) for 30 minutes on ice. In the peptide pulsed control, HCC cells were pulsed with 1 μ g/mL of the indicated peptides for 1 hour at 37°C . CD8+ T cells were then co-cultured with the pulsed HCC cell lines for 5 hours in the presence of 10 μ g/mL of Brefeldin A before intracellular staining was performed as described previously.

All acquisitions were done using BD LSR-II flow Cytometer and data were analyzed in Kaluza (Beckman Coulter, Brea, CA).

TCR-like Antibody Staining

HLA-A0201⁺ TCR-like antibody specific to HBV Env183-191¹ was used to quantify the cell surface expression of HLA-A0201/HBV-peptide specific complexes. HCC lines were pretreated with 1000 IU/mL of recombinant human

IFN- γ for 16 to 24 hours before harvest. As a positive control, HCC lines were pulsed with Env183–191 peptide at 1 $\mu\text{g}/\text{mL}$ for 1 hour at 37°C. Harvested cells were stained with the TCR-like antibodies at 1:100 for 1 hour on ice, followed by secondary staining with goat anti-mouse APC at 1:200 (#A865; Life technologies). This was followed by 2 rounds of APC amplification using the APC FASER amplification kit (Miltenyi, Bergisch Gladbach, Germany) and cells were fixed in 1% formaldehyde. Data acquisition was performed using the Amnis ImageStream MKII (Luminex, Austin, TX) and data were analyzed in the IDEAS (Luminex, Austin, TX).

HBV-specific CD8⁺ T-cell Clones

Four HLA-A0201 CD8⁺ T-cell lines specific for HBV epitopes Core 18–27, Envelope 183–191, Polymerase 455–463, or the influenza M1 58–66 were generated from HLA-A0201⁺ patients with acute hepatitis infection or from healthy donors as described previously.² T-cell lines were grown for 10 to 20 days in AIM-V+2% human AB serum (Sigma-Aldrich) supplemented with 20 IU/mL recombinant human interleukin (IL)-2 and 10 ng/mL IL-7 and IL-15 (Miltenyi Biotech).

HBV-specific T-cell Immunotherapy of Patients With HCC Relapses Post Liver Transplantation: Clinical History of Patients Treated With HBV-specific TCR T Cells

Patient 1. The patient at the time of liver transplantation was a 56-year-old Chinese man with chronic HBV infection and Child's A liver cirrhosis complicated by a right liver lobe HCC. There was no evidence of extrahepatic spread and he underwent living donor liver transplantation in December 2015 (Figure 4A). His postoperative course was uneventful and in July 2016, surveillance imaging revealed multiple pulmonary and abdominal metastases while his liver graft remain cancer free till date (Figure 4A). He was placed on Sorafenib treatment but repeat imaging in September and December 2016 demonstrated a worsening disease with rapidly enlarging pulmonary metastases and rising AFP levels (Figure 4A and 4C). The patient remained on Tacrolimus and mycophenolate mofetil immunosuppression for the entire duration of the therapy. He is also on long-term Entecavir treatment to suppress HBV replication and HBsAg was not detected in the serum before start of T-cell immunotherapy.

Patient 2. The patient at the time of liver transplantation was a 45-year-old Chinese man with chronic HBV infection. He underwent deceased donor liver transplantation in December 2013 and presented with multifocal HCC recurrence in December 2014 (Figure 4B). From the first presentation of HCC recurrence at the right iliac bone till date, he has received a series of radiotherapy, transarterial chemoembolization, FOLFOX chemotherapy, and multikinase inhibitors Lenvatinib and Regorafenib (Figure 4B). Even with the aggressive treatments, his disease continued to worsen with multiple new metastases detected in the lung, liver, bone, rectum,

adrenal gland, and peritoneum (Figure 4B and D). The patient remained on Sirolimus immunosuppression for the entire duration of the therapy and he is on long-term Entecavir treatment to suppress HBV replication. HBsAg was also undetectable in the serum before T-cell immunotherapy.

Engineering and Infusion of HBV-specific TCR T Cells

Production of HBV-specific TCR T cells for infusion is similar to that described previously.³ In brief, the required mRNA was in vitro transcribed using the mMessage mMachine T7 Ultra Kit (Ambion, Austin, TX) according to the manufacturer's instructions. The resulting product was concentrated by lithium chloride precipitation and redissolved in T4 buffer (BTX, Holliston, MA). Peripheral blood mononuclear cells (PBMCs) from the patient were isolated by Ficoll density gradient centrifugation, followed by activation for 8 days with 600 IU/mL of GMP grade IL-2 (Miltenyi) and 50 ng/mL of GMP grade OKT-3 (Miltenyi) in cell therapy grade AIM-V (Invitrogen) supplemented with 5% CTS Serum Replacement (Invitrogen). Activated T cells were then electroporated using the AgilePulse Max system (BTX) according to the manufacturer's recommended protocol. After electroporation, cells were left to rest overnight in AIM-V+5% CTS Serum Replacement + 100 IU/mL IL-2 at 37 °C and 5% CO₂. Quality control experiments were then performed to characterize HBV-specific TCR expression levels and function of the engineered T cells before infusion into the patient in 5% Albutein (Grifols, Barcelona, Spain).

Quality Control of Engineered HBV-specific T Cells

T-cell growth, electroporation efficiency, and function of TCR-redirected T cells were characterized for every infusion in both patients. T-cell growth was monitored by quantifying the T-cell numbers at the beginning of the in vitro expansion and after 8 days of activation by the trypan blue exclusion assay. Electroporation efficiency was quantified by staining with the appropriate TCR-V β antibodies (Beckman Coulter). To characterize the TCR T-cell function, EBV B cells expressing the appropriate HLA molecules were first pulsed with 1 $\mu\text{g}/\text{mL}$ of the corresponding peptides for 1 hour at 37°C. The TCR T cells were then co-cultured with the pulsed EBV B cells overnight in the presence of 2 $\mu\text{g}/\text{mL}$ Brefeldin A before intracellular staining was performed as described previously.

Biochemical, Virological, Imaging, and Serum Cytokine/Chemokine Analysis of Treated Patients

All biochemical, virological, and imaging analysis was performed by the Singapore General Hospital in accordance to their standard operating procedures for each assay requested. For serum cytokine/chemokine analysis, serum from patients was collected and analyzed using the 41-plex human cytokine bead-based assay (Millipore) according to the manufacturer's instructions.

Phenotypic Analysis of PBMCs

PBMCs of the patient were obtained before and on day 6 and 14 postinjection of 10×10^6 /kg of TCR-redirected T cells and were cryopreserved. For phenotypic analysis by mass cytometry (CyTOF), purified antibodies lacking carrier proteins were conjugated with heavy metals according to the protocol provided by Fluidigm. PBMCs were thawed and washed in RPMI, 10% fetal calf serum. Cells were stained with cisplatin for viability in phosphate-buffered saline for 5 minutes as described previously.⁴ Cells were then incubated with a surface marker antibody cocktail including the activation marker HLA-DR for 15 minutes on ice. Subsequently, cells were fixed and permeabilized with the FoxP3 staining kit (eBioscience) for intranuclear staining of Ki67 (30 minutes in perm buffer). After 2 washing steps, cells were stained for barcoding, fixed in phosphate-buffered saline 2% paraformaldehyde overnight, and stained for DNA.

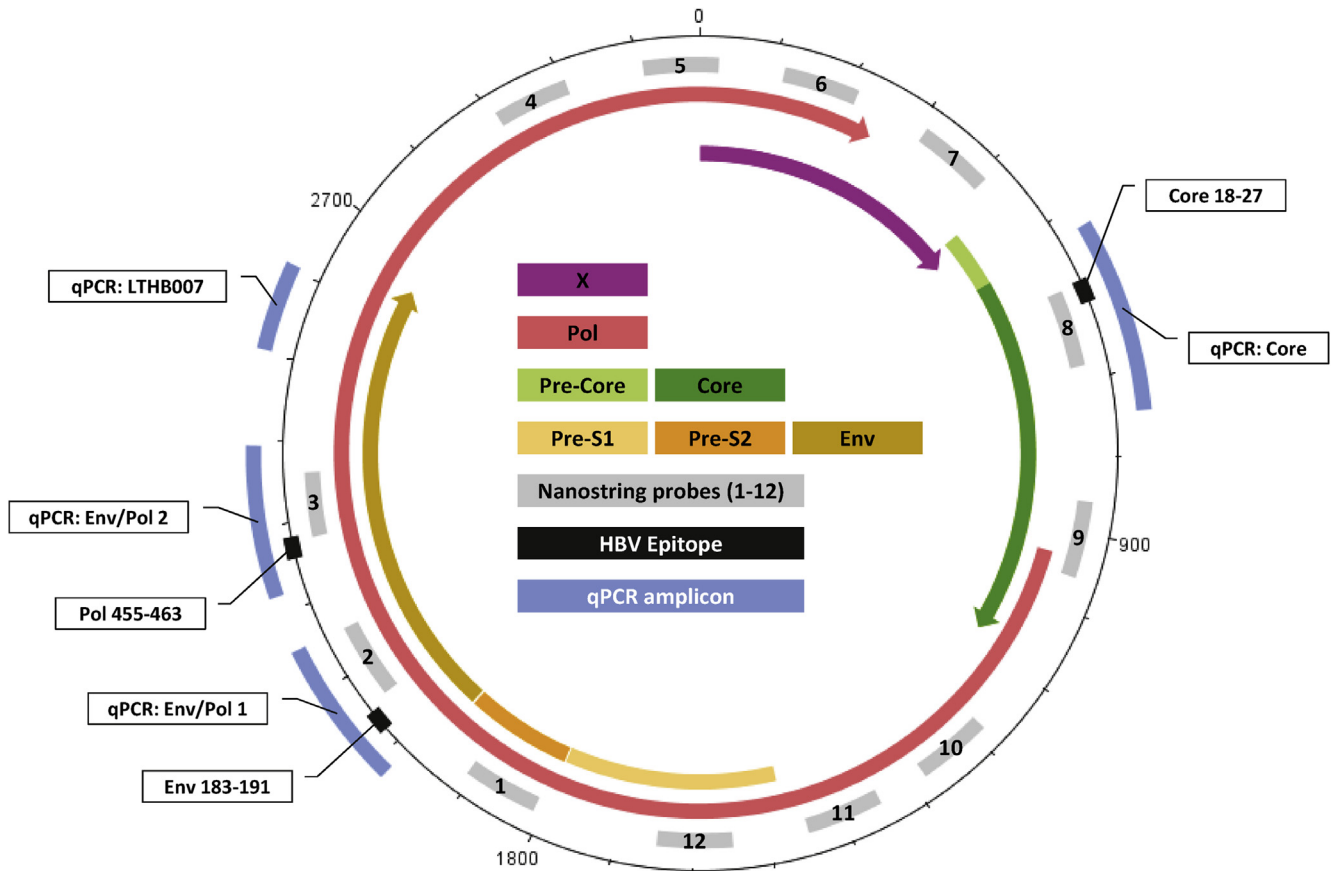
Data Analysis

After CyTOF acquisition (Helios, Fluidigm, South San Francisco, CA), an R script was applied to randomize any

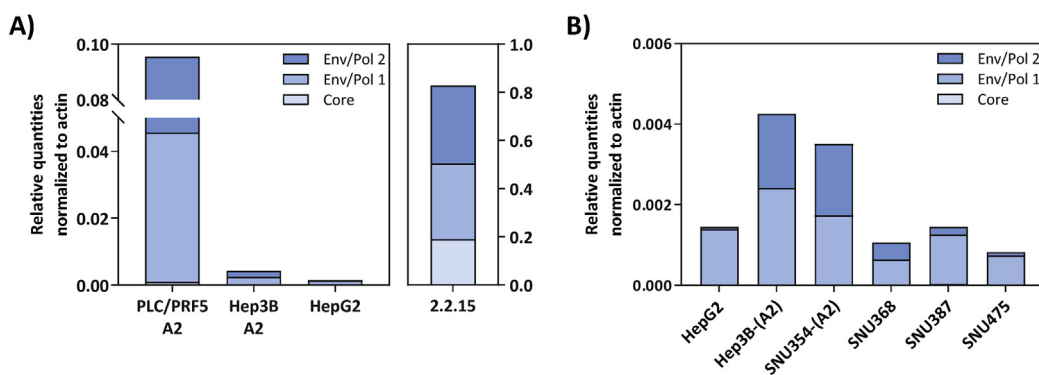
zero values using a uniform distribution of values between zero and -1 . The signal of each parameter was then normalized based on the EQ beads (Fluidigm). Cells were manually de-barcoded and analyzed with FlowJo (Tree Star, Ashland, OR).

References

1. Sastry KS, Too CT, Kaur K, et al. Targeting hepatitis B virus-infected cells with a T-cell receptor-like antibody. *J Virol* 2011;85:1935–1942.
2. Gehring AJ, Sun D, Kennedy PT, et al. The level of viral antigen presented by hepatocytes influences CD8 T-cell function. *J Virol* 2007;81:2940–2949.
3. Koh S, Shimasaki N, Suwanarusk R, et al. A practical approach to immunotherapy of hepatocellular carcinoma using T cells redirected against hepatitis B virus. *Mol Ther Nucleic Acids* 2013;2:e114.
4. Simoni Y, Fehlings M, Klooverpris HN, et al. Human innate lymphoid cell subsets possess tissue-type based heterogeneity in phenotype and frequency. *Immunity* 2017; 46:148–161.

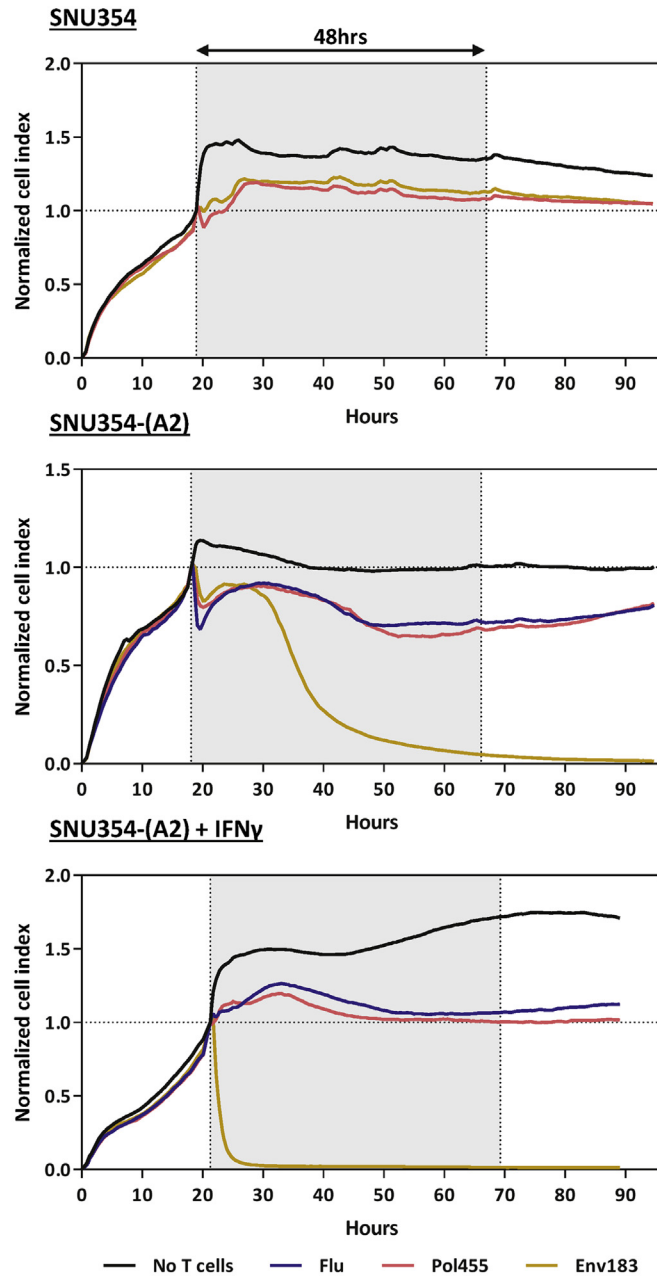


Supplementary Figure 1. Circular map of the overlapping open reading frames of HBV and the relative positions of the custom Nanostring probes, HBV epitopes, and qPCR amplicons. The open reading frames of HBV are shown in the corresponding colors. Custom-order Nanostring probes were designed to cover the entire HBV genome, but probes recognizing the ~2400–2800-bp region could not be produced within the manufacturer’s specifications and are omitted. *Black* segments denote the region of the HBV genome that encodes for HBV epitopes recognized by the Core18–27, Env183–191, and Pol455–463 TCRs. qPCR amplicons generated by the corresponding HBV-specific qPCR primer pairs are denoted in *blue*.



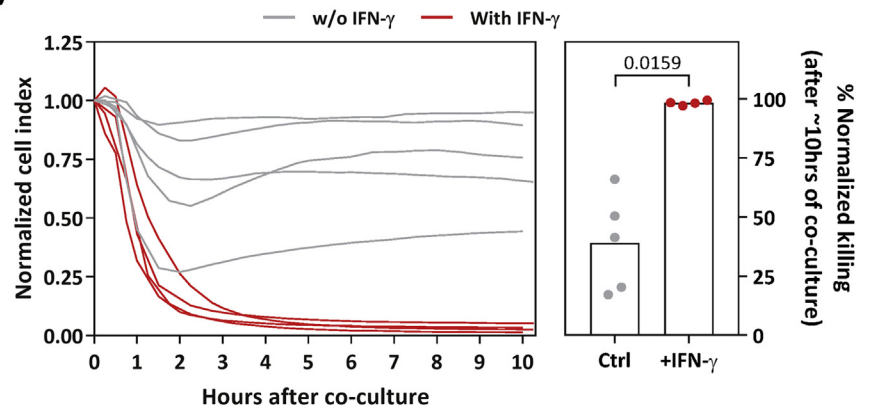
Supplementary Figure 2. Detection of HBV mRNA in HBV-HCC lines by qPCR. qPCR primer pairs specific to different parts of the HBV genome (Core, Env/Pol 1, and Env/Pol 2; see Figure 1) were used to quantify the relative expression of HBV mRNA in different HBV-HCC lines. Quantified values were normalized to actin housekeeping control. HepG2.215 and PLC/PRF5-(A2), both with higher relative quantities of HBV mRNA, were plotted in (A), whereas other HBV-HCC lines with lower relative quantities are shown in (B).

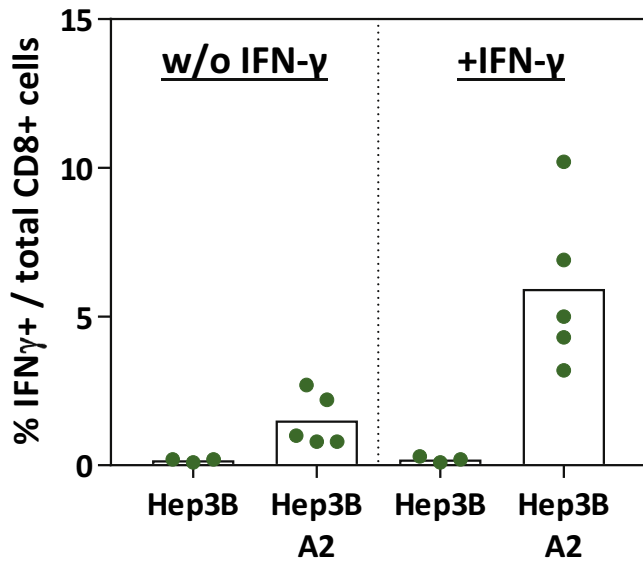
A)



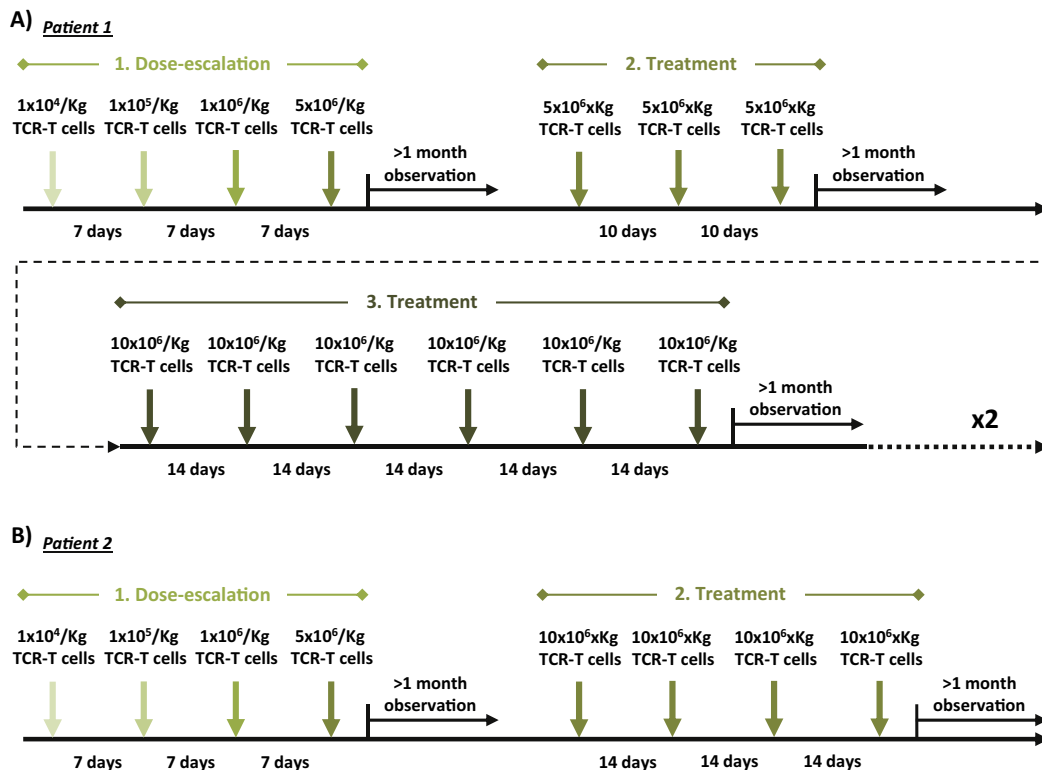
Supplementary Figure 3. xCelligence impedance-based cytotoxicity assay of IFN- γ pretreated SNU354-(A2) HBV-HCC lines. (A) Representative normalized cell index curves are shown. SNU354-(A2) lines were left untreated (*middle*) or pretreated with 1000 IU/mL IFN- γ overnight (*bottom*) before co-culturing with the Env183-191 (*brown*), Pol455-463 (*pink*), or Influenza M1 58-66 (*blue*) T-cell clones. Wells without T-cell lines (*black*) were included as controls. Normalized cell index curves obtained from control non-HLA-A2 expressing SNU354 lines are also shown (*top*). Cell indexes were normalized to the time when T cells were added and *shaded areas* indicate a 48-hour duration post T-cell addition. (B) Normalized cell index curves from the first 10.5 hours of co-culture with T cells (*left*). Each *red line* represents independent experiments with IFN- γ pretreated SNU354-(A2) lines, and experiments with untreated SNU354-(A2) lines are shown in *gray*. Killing of HBV-HCC lines at 10 hours post T-cell addition were summarized (*right*). Target killing was normalized to the wells with only SNU354 lines cultured (spontaneous target death). Bars show the average normalized killing and each *dot* represents a single experiment.

B)



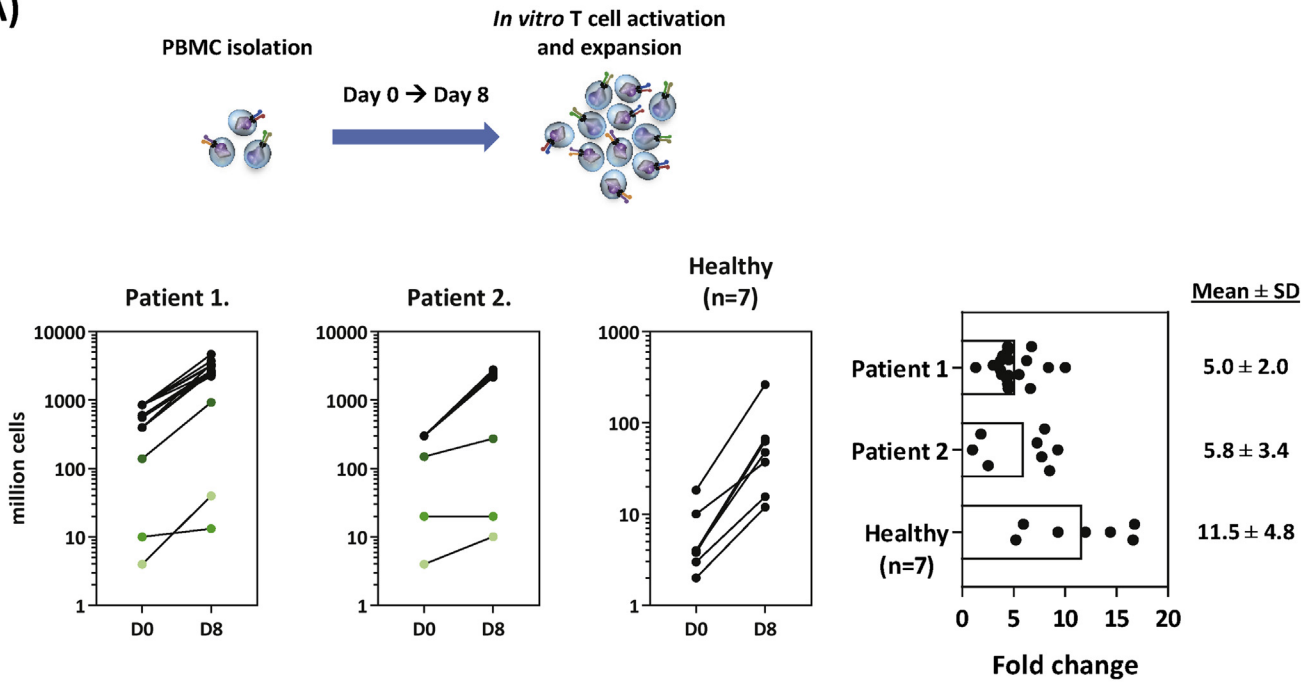


Supplementary Figure 4. Intracellular IFN- γ staining of Pol455–463 T cells activated by Hep3B-(A2) cells. Activation of Pol455–463 T cells was evaluated in the presence (*right*) and absence (*left*) of 1000 IU/mL of IFN- γ . Non-HLA-A2 expressing Hep3B cells are shown as controls. Each dot represents a single experiment.

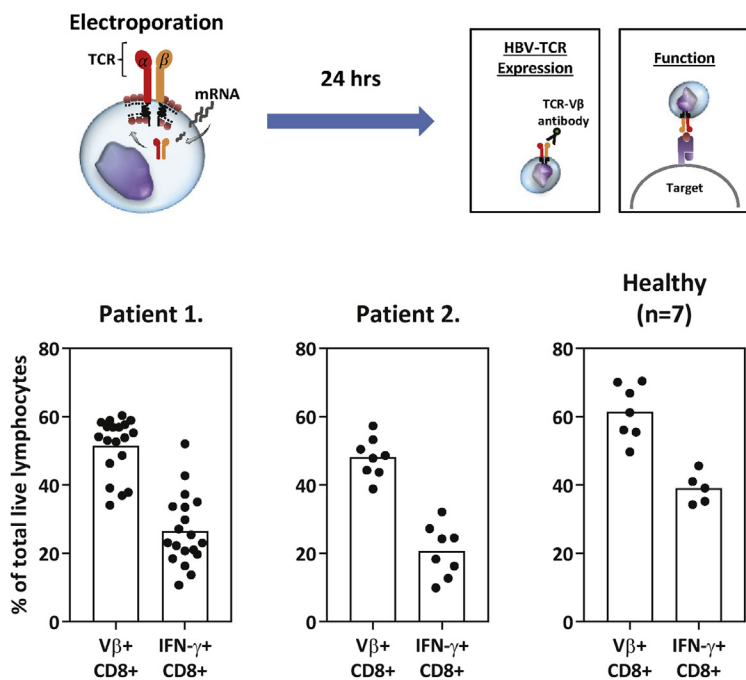


Supplementary Figure 5. Infusion schedule for both HBV-HCC patients treated with HBV-specific TCR T cells. The TCR T-cell infusion schedules for patient 1 (A) and patient 2 (B) are shown.

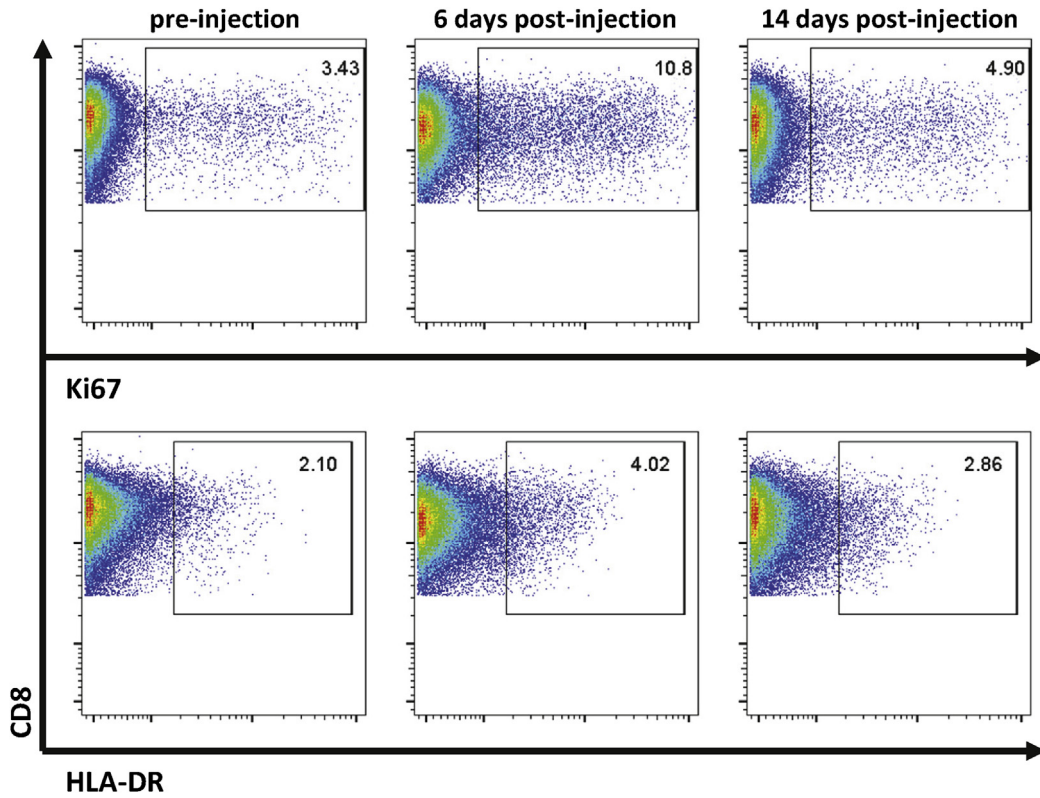
A)



B)



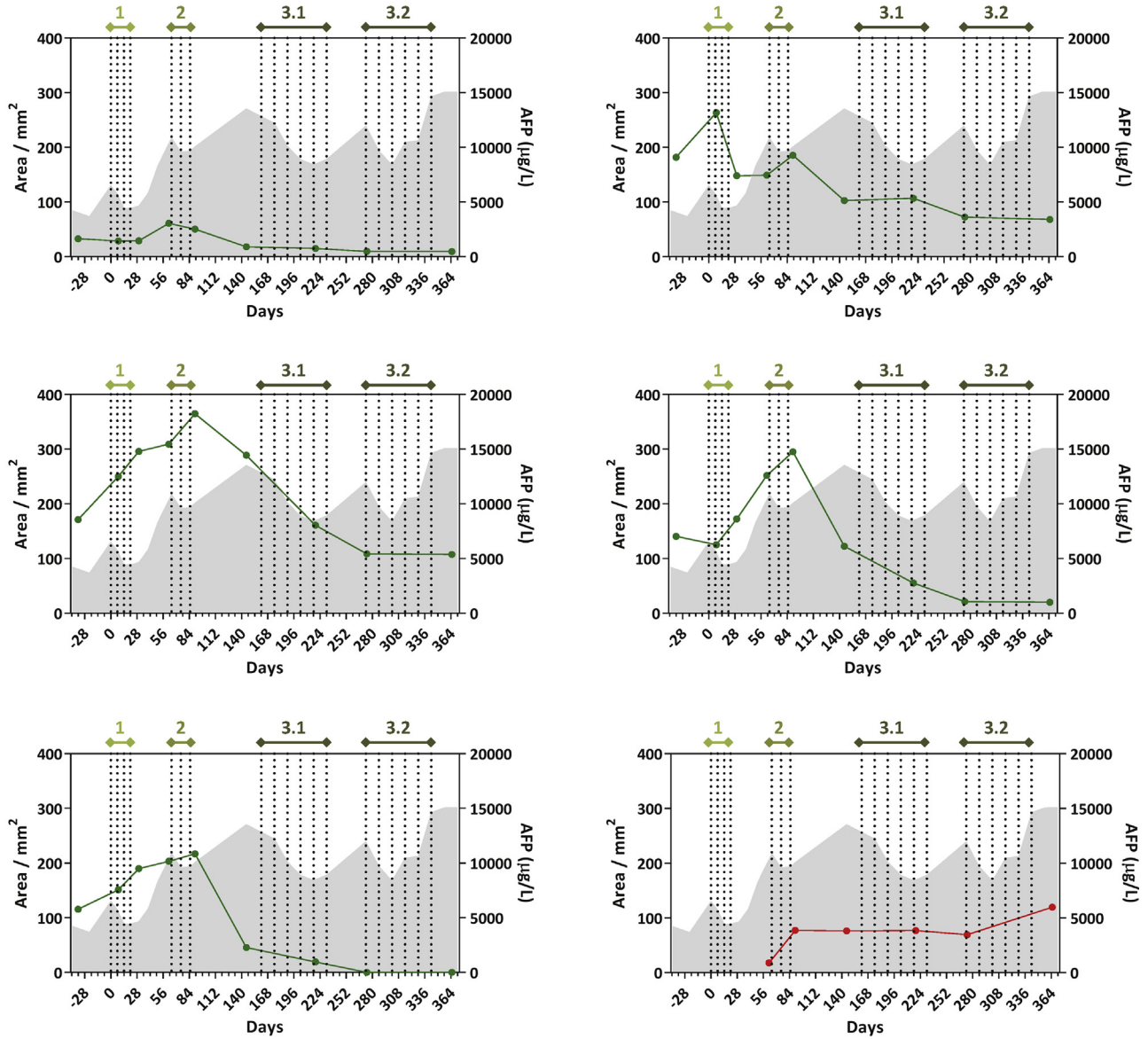
Supplementary Figure 6. In vitro expansion characteristics and function of TCR T cells engineered from both patients. (A) In vitro growth of T cells required for every infusion in both patients was monitored after 8 days of in vitro activation. The fold change in cell numbers are shown in the *right-most panel*. (B) TCR expression and function of TCR-redirection T cells were also quantified before each infusion in both patients. Each *dot* represents data obtained from T cells associated with a single infusion. Data from the engineering of T cells expanded from healthy donors (n = 7) were also included for comparison. Each *dot* represents a single donor.



Supplementary Figure 7. Temporary elevation of proliferating and activated CD8+ T cells in the circulation post TCR T-cell injection. PBMCs of the patient were obtained before and on days 6 and 14 post injection of 10×10^6 /kg of TCR-redirected T cells and analyzed for expression of markers of T-cell proliferation (Ki67) and activation (HLA-DR). Live CD8+ T cells were gated and the percentage of Ki67+ (*top*) and HLA-DR+ (*bottom*) cells is shown.

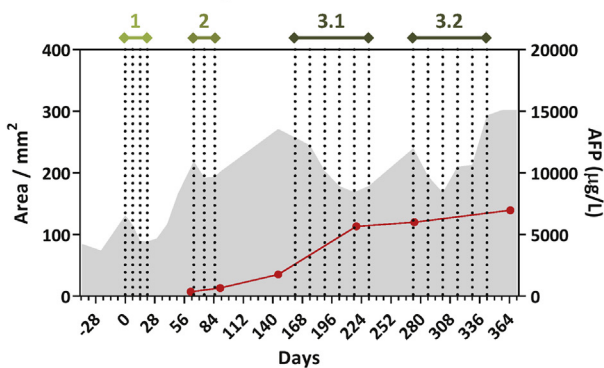
A)

Pulmonary metastases



B)

Retroperitoneal metastasis



Supplementary Figure 8. Cross-sectional area of the tumor nodules detected in the lungs and the retroperitoneal nodule in patient 1. The largest cross-sectional area of all tumor nodules in the lungs (A) and a single retroperitoneal nodule (B) were measured at specific intervals during the therapy. Vertical dotted lines denote each TCR T-cell infusion and the different phases of the treatment are indicated. Gray shaded areas represent the serum AFP concentrations.